Journal of Medicinal Chemistry Article

J. Med. Chem. **2009,** *52,* 6369–6381 **6369**
DOI: 10.1021/jm901018f

Synthesis, Kinase Inhibitory Potencies, and in Vitro Antiproliferative Evaluation of New Pim Kinase Inhibitors†

Rufine Akué-Gédu,[‡,§] Emilie Rossignol,[‡,§] Stéphane Azzaro,[‡,§] Stefan Knapp,[∥,⊥] Panagis Filippakopoulos,[∥] Alex N. Bullock,[∥] Jenny Bain,[#] Philip Cohen,[#] Michelle Prudhomme,[‡,§] Fabrice Anizon,*[,‡,§] and Pascale Moreau[‡,§]

[‡]*Clermont Université, Université Blaise Pascal, Laboratoire SEESIB, F-63177 Aubière, France,* [§]*CNRS, UMR6504, F-63177 Aubière, France,* [∥]*Structural Genomics Consortium, University of Oxford, Old Road Campus Building, Roosevelt Drive, Oxford OX3 7DQ, U.K.,* [⊥]*Department of Clinical Pharmacology, University of Oxford, Old Road Campus Building, Roosevelt Drive, Oxford OX3 7DQ, U.K., and* [#]*MRC Protein Phosphorylation Unit, College of Life Sciences, Sir James Black Centre, University of Dundee, Dundee DD1 5EH, Scotland, U.K.*

Received May 12, 2009

Members of the Pim kinase family have been identified as promising targets for the development of antitumor agents. After a screening of pyrrolo[2,3-*a*]- and [3,2-*a*]carbazole derivatives toward 66 protein kinases, we identified pyrrolo[2,3-*a*]carbazole as a new scaffold to design potent Pim kinase inhibitors. In particular, compound **9** was identified as a low nM selective Pim inhibitor. Additionally, several pyrrolo[2,3-*a*]carbazole derivatives showed selectivity for Pim-1 and Pim-3 over Pim-2. In vitro antiproliferative activities of **9** and **28**, the most potent Pim inhibitors identified, were evaluated toward three human solid cancer cell lines (PA1, PC3, and DU145) and one human fibroblast primary culture, revealing IC_{50} values in the micromolar range. Finally, the crystal structure of Pim-1 complexed with lead compound **9** was determined. The structure revealed a non-ATP mimetic binding mode with no hydrogen bonds formed with the kinase hinge region and explained the selectivity of pyrrolo-[2,3-*a*]carbazole derivatives for Pim kinases.

Introduction

Serine/threonine kinases of the Pim family (Provirus integration site for Moloney murine leukemia virus[a]) are encoded by the *pim* proto-oncogenes.[1−3] The first member of the family, *pim-1*, was originally identified as a common proviral insertion site in Moloney murine leukemia virus-induced T-cell lymphomas in mice.[4] In humans, three Pim family members (Pim-1, Pim-2, and Pim-3) have been identified which share 60−70% sequence identity in their kinase domains.[5] Pim kinases have been reported to be implicated in various signaling pathways and play key roles regulating cell cycle progression and apoptosis. Pim kinases are overexpressed in many cancer types and are believed to play a role in the initiation and progression of the malignant phenotype. In particular, Pim-1 and Pim-2 have been reported to be highly expressed in leukemia, lymphoma, prostate cancer, and multiple myeloma.[6−14] Moreover, it has been shown that Pim-2 overexpression promotes growth-factor independent survival of hematopoietic cell lines.[11] A number of studies also reported aberrant expression of Pim-3 in pancreas and colon cancer and suggested an involvement of Pim-3 in gastric adenoma-adenocarcinoma transition and subsequent invasion and metastasis.[15−18] Furthermore, it has been established that Pim kinases are implicated in the development of resistance to tyrosine kinase inhibitors[19] and to the mTOR inhibitor rapamycin.[20,21] These findings suggest that Pim kinases may be relevant anticancer drug targets and established synthesis of Pim inhibitors as an attractive area of chemical biology. Only a few selective Pim kinase inhibitors, targeting mainly Pim-1 and Pim-2, have been described in the literature so far but an increasing number of recent publications reporting the identification of new and selective Pim kinase inhibitors indicate a growing interest in this field. As illustrated in Figure 1, these inhibitors present a high degree of chemical diversity. Quercetagetin **I** is a flavonoid of submicromolar inhibitory activity toward Pim-1.[22] In contrast to the

†The structure of the cocrystal **9**/Pim-1 have been deposited in the PDB with accession code 3JPV.

*To whom correspondence should be addressed. Phone: +33 (0) 4 73 40 53 64. Fax: +33 (0) 4 73 40 77 17. E-mail: Fabrice.ANIZON@univ-bpclermont.fr.

[a] Abbreviations: AMPK, AMP-activated protein kinase; ATF2, activating transcription factor 2; ATP, adenosine triphosphate; BRSK, brain-specific kinase; CaMK, calmodulin-dependent kinase; BSA, bovin serum albumin; CaMKK, CaMK kinase; CDK, cyclin-dependent protein kinase; CHK, checkpoint kinase; CK, casein kinase; CSK, C-terminal Src kinase; DDQ, 2,3-dichloro-5,6-dicyano-*p*-benzoquinone; DMF, dimethylformamide; DTT, dithiothreitol; EF2K, elongation-factor-2 kinase; EGTA, ethylene glycol-bis(2-aminoethylether)-*N*,*N*,*N*′,*N*′-tetraacetic acid; ERK, extracellular-signal-regulated kinase; GSK3, glycogen synthase kinase 3; GST, glutathione transferase; HIPK, homeodomain-interacting protein kinase; His_6, hexahistidine; IKK, inhibitory κB kinase; JNK, c-Jun N-terminal kinase; Lck, lymphocyte cell-specific protein-tyrosine kinase; MAPK, mitogen-activated protein kinase; MAPKAP-K, MAPK-activated protein kinase; MARK, microtubule-affinity-regulating kinase; MBP, myelin basic protein; MELK, maternal embryonic leucine-zipper kinase; MKK1, MNK, MAPK-integrating protein kinase; MSK, mitogen- and stress-activated protein kinase; MST, mammalian homologue Ste20-like kinase; NEK, NIMA (never in mitosis in *Aspergillus nidulans*)-related kinase; PAK, p21-activated protein kinase; PDK, 3-phosphoinositide-dependent protein kinase; PHK, phosphorylase kinase; PIM, provirus integration site for Moloney murine leukemia virus; PKA, cAMP-dependent protein kinase; PKB, protein kinase B (also called Akt); PKC, protein kinase C; PKD, protein kinase D; PLK, polo-like kinase; PPSE, polyphosphoric acid trimethylsilyl ester; PRAK, p38-regulated activated kinase; PRK, protein kinase C-related kinase; ROCK, Rho-dependent protein kinase; RSK, p90 ribosomal S6 kinase; S6K1, S6 kinase 1; Sf21, *Spodoptera frugiperda* (fall armyworm) 21; SGK, serum- and glucocorticoid-induced kinase; SmMLCK, smooth-muscle myosin light-chain kinase; Src, sarcoma kinase; SRPK, serine-arginine protein kinase; mTOR, mammalian target of rapamycin; TFA, trifluoroacetic acid.

Published on Web 09/29/2009

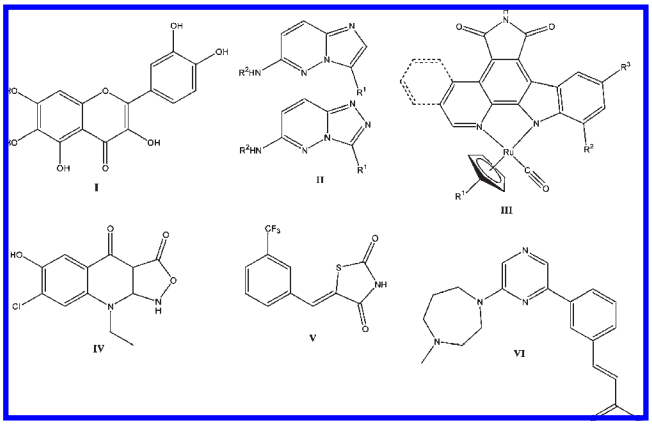

Figure 1. Some of the Pim kinase inhibitors described recently in the literature.

moderate inhibitory activity of quercetagetin, a potent and selective Pim-1 inhibitory activity of nanomolar potency was identified in substituted imidazo[1,2-*b*]- and triazolo[4,3-*b*]-pyridazines series[23,24] (**II**) and highly potent organoruthenium derivatives **III**.[25,26] In addition, isoxazolo[3,4-*b*]quinoline-dione **IV** have been reported as a nanomolar Pim-1 and Pim-2 inhibitor with a high degree of selectivity[27] and the thiazolidine derivative **V** has micromolar potency for these two kinases.[28] Finally, compound **VI** and its analogues have recently been reported to be a new class of selective Pim-1 and Pim-2 inhibitors with nanomolar potencies.[29] As part of our ongoing studies concerning the design of new anticancer agents, we are particularly interested in novel polyheterocyclic scaffolds with kinase inhibitory potencies and in vitro antiproliferative activities. Here, we focused on the synthesis of a series of pyrrolocarbazoles and in particular the preparation of pyrrolo[2,3-*a*]- and [3,2-*a*]carbazole derivatives. Apart from recent work by Fousteris et al. that disclosed an example of pyrrolo[2,3-*a*]carbazole derivative as a modest inhibitor of CDK1,[30] pyrrolocarbazoles have not been identified as potent and selective kinase inhibitors so far. In this study, we report our efforts adopting the pyrrolo[2,3-*a*]carbazole scaffold for the development of potent and novel Pim kinase inhibitors. Finally, an X-ray structure of a cocrystal of Pim-1 in complex with our lead compound was solved, revealing its ATP competitive but not mimetic binding mode.

Synthesis and Kinase Inhibitory Activity. To identify new scaffolds for the design of new kinase inhibitors, we started our study from the pyrrolo[3,2-*a*]- and [2,3-*a*]carbazoles **5** and **7** (Scheme 1), which were described for the first time more than 20 years ago.[31,32] Pyrrolo[3,2-*a*]carbazole **5** or substituted derivatives were synthesized either by Pd cross-coupling,[33] Fischer indole synthesis,[34] or using photochemistry.[35,36] Substituted pyrrolo[2,3-*a*]carbazoles have been recently synthesized by Stamos and Nikolaropoulos.[30,37]

Our approach to access these structures was a Fischer indolization from tetrahydroindolone **2** and phenylhydrazine in acetic acid (Scheme 1). Poor yield and purification difficulties led us to protect the nitrogen atom of compound **2** with a benzenesulfonyl group. Starting from protected derivative **1**,[38] pyrrolocarbazole **4** was isolated in 24% yield. Deprotection using sodium hydroxide in methanol led to **5** in 96% yield. Comparatively, compound **6** and **7** were prepared from **3**[39] in 17% and 92% yields, respectively, for Fischer indolization and deprotection steps. Formylation of compounds **5** and **7** was carried out using oxalyl chloride and

Scheme 1. Synthesis of Pyrrolo[2,3-*a*]- and [3,2-*a*]carbazoles[a]

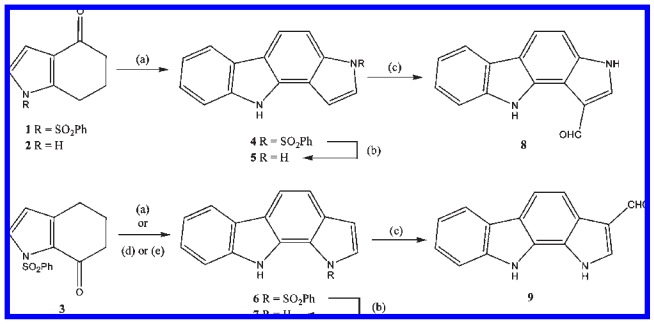

[a] Reagents and conditions: (a) $PhNHNH_2$, AcOH, **4** = 24%, **6** = 17%; (b) NaOH, MeOH, **5** = 96%, **7** = 92%; (c) (i) $(COCl)_2$, DMF, CH_2Cl_2, (ii) aq NaOH, **8** = 66%, **9** = 65%; (d) (i) $PhNHNH_2$, PPSE, CH_3NO_2, (ii) DDQ, 36%; (e) (i) $PhNHNH_2$, choline chloride-$ZnCl_2$ 1:2, (ii) DDQ, EtOAc, 78%.

DMF in CH_2Cl_2, leading to **8** and **9** in 66% and 65% yields, respectively.

At this stage, we undertook a screen of compounds **5**, **7**, **8**, and **9** toward a panel of protein kinases. Compounds were tested at 10 μM toward 66 protein kinases, using an assay described by Bain et al.[40] The results are shown as the percentage of remaining activity in the presence of an inhibitor compared with the control incubations in the absence of inhibitor (Table 1). No significant activity was found for pyrrolo[3,2-*a*]carbazoles **5** and **8**. These two compounds induced less than 30% of enzyme inhibition with all kinases tested, except for compound **5**, causing 53% inhibition of ERK8 and 71% inhibition of Pim-1, and for compound **8**, inducing 64% inhibition of CaMK1. Conversely, we were pleased to notice that compound **9** was a potent and selective inhibitor of Pim kinases, with an inhibition of enzymatic activity of 98% for Pim-1, 93% for Pim-2, and 99% for Pim-3. Furthermore, unsubstituted compound **7** was slightly active toward Pim-1 and Pim-3 kinases, with an inhibition of enzymatic activity of 80% and 62%, respectively.

These preliminary results encouraged us to perform the synthesis of new pyrrolo[2,3-*a*]carbazole derivatives. When compared to **7**, compound **9** is bearing a formyl group at the C-3 position, which positively contributes to the Pim kinase inhibition (compare **7** and **9**). We expected that the introduction of various substituents at this position would lead to compounds of increased inhibitory potency. Nevertheless, the poor yield obtained for the synthesis of compound **7** was detrimental to the overall synthesis efficiency. The methods used to optimize the Fischer indolization step are outlined in Scheme 1. We first tried the use of polyphosphoric acid trimethylsilyl ester (PPSE) for the indolization followed by the use of DDQ for the aromatization, as described by Fousteris et al.[37] for the preparation of pyrrolo[2,3-*a*]-carbazole substituted at the C-2 position by an ethoxycarbonyl group. Using this method, the yield of preparation of **6** from **3** was increased 2-fold from 17% to 36%. Nevertheless, this yield was not satisfying and the use of dangerous nitromethane prompted us to find other conditions. Recent work by Xu et al. has related the use of ionic liquid for Fischer indole synthesis.[41] We then decided to experiment this ionic liquid method by the use of the easy accessible choline chloride-zinc chloride 1:2 ionic liquid. A mixture of phenyl hydrazine and **3** in this ionic liquid was heated at 120 °C and subjected to DDQ oxidation in a one-pot procedure, to give **6** in a higher 78% yield.

Table 1. Residual Activities (%) at 10 μM for Compounds **5** and **7**−**9**

	compd			
kinases	**5**	**7**	**8**	**9**
MKK1	75 ± 6	87 ± 37	104 ± 14	50 ± 7
ERK1	97 ± 18	108 ± 9	95 ± 9	87 ± 13
ERK2	100 ± 10	94 ± 11	94 ± 13	92 ± 8
JNK1	116 ± 2	102 ± 11	113 ± 2	102 ± 7
JNK2	130 ± 9	118 ± 10	111 ± 7	128 ± 8
JNK3	111 ± 0.4	108 ± 3	96 ± 4	113 ± 8
p38α MAPK	115 ± 14	108 ± 6	108 ± 9	102 ± 23
P38β MAPK	91 ± 4	100 ± 13	96 ± 4	80 ± 9
p38γ MAPK	111 ± 7	111 ± 13	109 ± 2	74 ± 10
p38δ MAPK	89 ± 9	78 ± 4	83 ± 4	92 ± 0.5
ERK8	47 ± 16	55 ± 6	112 ± 38	20 ± 2
RSK1	99 ± 11	105 ± 3	120 ± 22	38 ± 7
RSK2	107 ± 0.8	99 ± 2	78 ± 9	77 ± 5
PDK1	82 ± 3	86 ± 1	85 ± 10	76 ± 3
PKBα	110 ± 8	120 ± 4	112 ± 8	96 ± 1
PKBβ	107 ± 2	107 ± 0.2	107 ± 16	98 ± 6
SGK1	102 ± 1	82 ± 13	105 ± 4	64 ± 9
S6K1	87 ± 1	89 ± 2	82 ± 10	38 ± 2
PKA	96 ± 7	95 ± 2	83 ± 4	60 ± 12
ROCK2	89 ± 11	86 ± 2	86 ± 4	25 ± 2
PRK2	84 ± 8	95 ± 2	101 ± 16	31 ± 4
PKCα	103 ± 14	111 ± 27	95 ± 10	84 ± 17
PKCζ	87 ± 2	91 ± 7	91 ± 6	83 ± 1
PKD1	71 ± 3	83 ± 9	87 ± 2	28 ± 4
MSK1	94 ± 5	90 ± 2	84 ± 8	71 ± 1
MNK1	101 ± 7	69 ± 3	106 ± 6	27 ± 1
MNK2	103 ± 14	95 ± 6	109 ± 16	55 ± 2
MAPKAP-K2	95 ± 20	118 ± 12	95 ± 5	84 ± 0.2
MAPKAP-K3	88 ± 7	89 ± 3	90 ± 7	69 ± 0.5
PRAK	114 ± 12	97 ± 2	114 ± 7	72 ± 4
CAMKKα	92 ± 8	76 ± 4	90 ± 4	42 ± 3
CAMKKβ	87 ± 6	93 ± 4	102 ± 0.2	56 ± 4
CaMK1	80 ± 5	29 ± 11	36 ± 0.3	71 ± 4
smMLCK	82 ± 7	86 ± 12	91 ± 5	60 ± 12
PHK	71 ± 6	90 ± 2	88 ± 6	33 ± 8
CHK1	112 ± 6	123 ± 2	101 ± 7	97 ± 4
CHK2	73 ± 5	58 ± 8	89 ± 5	38 ± 4
GSK3β	102 ± 9	111 ± 2	96 ± 8	88 ± 5
CDK2-Cyclin A	95 ± 2	97 ± 1	109 ± 1	74 ± 9
PLK1	105 ± 7	111 ± 12	106 ± 6	91 ± 4
AURORA B	67 ± 0.1	67 ± 5	92 ± 1	68 ± 2
AURORA C	99 ± 6	85 ± 1	104 ± 0.3	79 ± 3
AMPK	79 ± 6	80 ± 2	85 ± 6	59 ± 3
MARK3	94 ± 8	116 ± 12	105 ± 5	88 ± 0.3
BRSK2	76 ± 8	58 ± 6	101 ± 6	22 ± 18
MELK	82 ± 20	93 ± 7	89 ± 19	61 ± 14
CK1	99 ± 1	107 ± 3	113 ± 1	103 ± 3
CK2	96 ± 21	91 ± 15	98 ± 17	62 ± 3
NEK2a	96 ± 5	104 ± 7	100 ± 2	88 ± 3
NEK6	71 ± 3	90 ± 6	86 ± 6	78 ± 11
NEK7	92 ± 3	96 ± 1	95 ± 1	89 ± 2
IKKβ	110 ± 32	106 ± 1	108 ± 14	71 ± 4
Pim-1	53 ± 0.1	20 ± 0.1	79 ± 4	2 ± 0.4
Pim-2	77 ± 5	62 ± 8	102 ± 1	7 ± 1
Pim-3	29 ± 3	38 ± 2	103 ± 7	1 ± 5
SRPK1	94 ± 10	90 ± 13	93 ± 16	84 ± 8
MST2	77 ± 1	82 ± 5	96 ± 8	63 ± 4
EF2K	92 ± 7	101 ± 7	105 ± 3	90 ± 14
HIPK2	72 ± 18	59 ± 7	95 ± 18	25 ± 4
HIPK3	106 ± 4	97 ± 1	100 ± 3	64 ± 4
PAK4	84 ± 9	84 ± 13	88 ± 13	88 ± 13
PAK5	99 ± 3	82 ± 10	96 ± 4	87 ± 1
PAK6	91 ± 2	92 ± 3	99 ± 8	94 ± 10
Src	102 ± 23	98 ± 18	99 ± 11	85 ± 20
Lck	81 ± 14	88 ± 14	114 ± 49	76 ± 1
CSK	72 ± 17	98 ± 11	87 ± 8	74 ± 5

This optimized procedure for the synthesis of the pyrrolo[2,3-*a*]carbazole scaffold made easier the preparation of new diversely substituted derivatives. We then followed up our investigations by the synthesis of pyrrolo[2,3-*a*]carbazoles diversely substituted at the C-3 position (Scheme 2). Reduction of **9** using $NaBH_4$ led to **10** in 67% yield. Carboxamide **11** and trifluoroacetyl derivative **12** were prepared from **7** using chlorosulfonylisocyanate and trifluoroacetic anhydride in 20% and 42% yields, respectively. Reaction of **7** with oxalyl chloride was carried out to prepare the acyl chloride intermediate **13**, which was directly used for the following step. Treatment of **13** with ethanol or diethylamine led respectively to the ester **14** in 73% yield and to amide **15** in 66% yield. Reduction of **14** was carried out with $LiAlH_4$ to give alcohol **16** in 72%. Reaction of **15** with hydroxylamine led to oxime derivative **17** in 19% yield.

To get insight on the influence of the substituents introduced at the C-3 position or the presence of a benzenesulfonyl group at the N-1 position, compounds **6**, **10**−**12**, **16**, and **17** were tested for their ability to inhibit Pim kinases at 10 and 1 μM (Table 2). Compared to compound **9**, no increase of inhibition was observed. Only compounds **11** and **12**, bearing carboxamido or trifluoroacetyl groups, exhibited a Pim kinase inhibition percentage higher than 90% at 10 μM. Compound **11** caused 91% inhibition of Pim-1 and Pim-3 at 10 μM. At the same concentration, compound **12** induced 93% inhibition of Pim-3 activity. The reduction of the formyl to a hydroxymethyl group (compound **10**) was detrimental to the inhibition potency, with a residual activity in the same range as the nonsubstituted pyrrolocarbazole **7**. Moreover, compound **6**, bearing a benzenesulfonyl group at the N-1 position, was only slightly active, with an enzymatic inhibition $<40\%$ against the three Pim kinases. All together, this first insight on the inhibition potencies of these derivatives indicates that the presence of a free indole nitrogen and of a strong hydrogen bond acceptor like a formyl group at the C-3 position seem to be required for good activity.

To carry on with the synthesis of new pyrrolo[2,3-*a*]carbazole analogues, we prepared new derivatives substituted at the C-7 position. Substitution at this position was easily accessible from *p*-bromophenylhydrazine. Reaction of *p*-bromophenylhydrazine with ketone **3** in ionic liquid followed by oxidation in the presence of DDQ led to compound **18** in 74% yield (Scheme 3). Deprotection was performed in NaOH/MeOH, leading to **19** in 92% yield. Various substituents were introduced via a Suzuki cross-coupling by reaction of **19** with several aryl boronic acids in the presence of $Pd(PPh_3)_2Cl_2$ and Na_2CO_3. Compounds **20**−**27** were isolated in 50−65% yields.

Formylation of **19** was carried out in the same conditions as that for the preparation of compound **9**, leading to **28** in 66% yield (Scheme 3). However, these conditions could not be applied to **20**−**27** for solubility problems. Therefore, the formylation of **20** was achieved at 120 °C in Vilsmeier conditions using $POCl_3$ and DMF, leading to the isolation of **29** in 45% yield. To shorten the reaction time, formylation of compounds **21**−**27** was performed under microwave irradiation. Carboxamides **29**−**35** were obtained in 30−67% yield. Unfortunately, a formylated analogue of **27** could not be isolated because of purification problems.

These new compounds **19**, **28**−**35** were tested toward Pim kinases at 10 and 1 μM (Table 2). Only three compounds were potent inhibitors, causing more than 90% of enzyme inhibition at 10 μM. At this concentration, when bromo

Scheme 2. Synthesis of Pyrrolo[2,3-*a*]carbazole Derivatives Substituted at the C-3 Position[a]

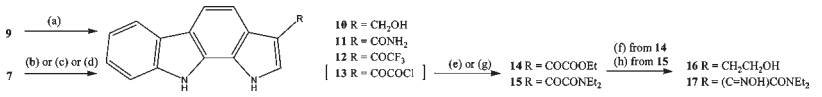

[a] Reagents and conditions: (a) $NaBH_4$, MeOH, 67%; (b) (i) $ClSO_2NCO$, CH_3CN; (ii) HCl, H_2O/THF, 20%; (c) $(CF_3CO)_2O$, DMF, 42%; (d) $(COCl)_2$, Et_2O; (e) EtOH, NEt_3, 73% from **7**; (f) $LiAlH_4$, dioxane, 72%; (g) Et_2NH, Et_2O, 66% from **7**; (h) NH_2OH, pyridine, 19%.

Table 2. Residual Activities (%) at 10 and 1 μM for Compounds **7**, **9**−**12**, **15**, **17**, **19**, and **28**−**35** (IC_{50} (μM) are Indicated in Parenthesis)

	Pim-1		Pim-2		Pim-3	
compd	10 μM	1 μM	10 μM	1 μM	10 μM	1 μM
6	61 ± 7	83 ± 5	62 ± 13	65 ± 12	64 ± 3	102 ± 4
7	20 ± 0		62 ± 8		38 ± 2	
9	2 ± 0		7 ± 1		1 ± 5	
	(0.12 ± 0.01)		(0.51 ± 0.23)		(0.01 ± 0.00)	
10	28 ± 2	72 ± 15	47 ± 18	46 ± 9	18 ± 2	68 ± 12
11	9 ± 0		27 ± 2		9 ± 7	
	(0.78 ± 0.02)				(0.21 ± 0.06)	
12	20 ± 3	61 ± 13	30 ± 1	54 ± 28	7 ± 3	20 ± 8
					(0.17 ± 0.05)	
16	35 ± 4	90 ± 5	50 ± 9	69 ± 4	21 ± 7	72 ± 8
17	41 ± 6	80 ± 3	27 ± 2	62 ± 9	21 ± 3	74 ± 2
19	12 ± 0	69 ± 4	46 ± 3	67 ± 15	8 ± 2	55 ± 11
					(0.44 ± 0.01)	
28	6 ± 2	31 ± 2	53 ± 7	82 ± 5	6 ± 0	11 ± 3
	(0.57 ± 0.04)				(0.04 ± 0.01)	
29	17 ± 3	64 ± 18	31 ± 3	65 ± 15	12 ± 1	46 ± 8
30	16 ± 1	60 ± 5	53 ± 1	68 ± 16	15 ± 0	54 ± 6
31	39 ± 7	69 ± 21	70 ± 8	67 ± 4	48 ± 6	77 ± 5
32	15 ± 2	65 ± 3	55 ± 2	72 ± 10	15 ± 1	54 ± 9
33	6 ± 1	39 ± 1	32 ± 5	59 ± 19	6 ± 1	26 ± 3
	(0.66 ± 0.18)				(0.20 ± 0.04)	
34	28 ± 0	79 ± 1	52 ± 6	49 ± 2	23 ± 1	70 ± 8
35	29 ± 1	68 ± 10	70 ± 23	73 ± 11	31 ± 2	77 ± 3

analogues **19** and **28** were evaluated, the percentages of residual enzymatic activity were found to be 12% and 6% for Pim-1 and 8% and 6% for Pim-3, respectively. As for compounds **7** and **9**, the presence of a formyl group at the C-3 position was favorable to the inhibitory potency. Conversely, the presence of an aryl group led to the smallest inhibitory potencies when compared with compounds **9** or **28**, except for compound **33** bearing a 2,4-difluorophenyl group at the C-7 position, inhibiting Pim-1 and Pim-3 kinases with a percentage of inhibition of 94%. While compounds **30** and **32**, bearing respectively phenyl and 4-fluorophenyl groups, exhibited similar and mild potencies toward the three Pim kinases, it appears that the increased inhibitory activity for compound **33** is due to the extra fluorine atom at the 2 position of the phenyl group.

Compounds that caused enzyme inhibition greater than 90% at 10 μM (compounds **9**, **11**, **12**, **19**, **28**, and **33**, Table 2) were used for the determination of IC_{50} values toward corresponding Pim kinases. All these compounds showed an IC_{50} value in the submicromolar range. The inhibitory potency was different considering the kinase tested. Our results suggest that the order of inhibitory potency for these new inhibitors was Pim-3 > Pim-1 > Pim-2. The best compound of the series against all the three Pim kinases was the formyl derivative **9**, with IC_{50} values of 0.01 μM for Pim-3, 0.12 μM for Pim-1, and 0.51 μM for Pim-2. Moreover, compound **28** exhibited a nanomolar inhibitory potency for Pim-3, with an IC_{50} value of 0.04 μM. Compound **28** was also active against Pim-1, with an IC_{50} value of 0.57 μM.

In Vitro Antiproliferative Activity. In vitro antiproliferative activities of **9** and **28** were examined by a fluorometric assay (resazurin reduction test) using one human fibroblast primary culture and three human solid cancer cell lines: PC3 and DU145 (prostate cancer cells) and PA1 (ovarian carcinoma) (Table 3). Whereas compound **9** exhibited the best inhibitory activity toward Pim kinases, compound **28** was found to be more active against the cell lines tested, possibly due to its improved cellular penetration. The best in vitro antiproliferative activity of compound **28** was found against PA1 cells, with an IC_{50} value of 2.8 μM. In addition, compound **28** exhibited an interesting potency against PC3 (IC_{50} value of 5.9 μM), which is known to express high level of Pim-1 kinase. Toward DU145 and fibroblast cell lines, in vitro antiproliferative activities of compound **28** were found to be in the same range, with IC_{50} values of 12.2 μM toward DU145 cell line and 11 μM toward fibroblast cells. In comparison to **28**, compound **9** was found to be less active. As for compound **28**, the higher potency of compound **9** was determined against the PA1 cell line, with an IC_{50} value of 4.5 μM. Toward the other cell lines, IC_{50} values were found to be in the range 10−30 μM, with the best potency against PC3 (IC_{50} value of 9.5 μM).

X-ray Structure Analysis. All the structure−activity relationship studies presented above were established without any structural insight on the mode of binding of this new series of Pim kinase inhibitors. Therefore, after the identification of our lead compound, we were interested to determine the binding mode and point out the interactions that would explain the high selectivity of this inhibitor for Pim kinases and its modest but significant selectivity for Pim-3. To accomplish this, compound **9**, the best active derivative in this series, was cocrystallized with Pim-1 kinase and the X-ray crystal structure was solved at 2.35 Å resolution. Statistics on data collection and refinement are summarized in Table 4. Compound **9** occupied the ATP-binding site of Pim-1. However, in contrast to typical ATP mimetic inhibitors, the planar pyrrolocarbazole scaffold was inserted into the ATP binding cleft with aromatic NH oriented away from the hinge region not forming hydrogen bonds with Glu121 or another backbone carbonyl of the Pim hinge region. Thus, binding of compound **9** is ATP competitive but not ATP mimetic (Figure 2). The aldehyde formed a hydrogen bond with the conserved active site lysine, Lys67. On the basis of the presence of a formyl group in the structure of these compounds, one could envisage the formation of a Schiff base with a primary amino group in the enzyme, stabilized by conjugation with the aromatic pyrrolocarbazole nucleus. Conversely, the carbonyl group could be considered to belong to a vinylogous formamide system, with the conjugated N-1 electron pair decreasing the electrophilicity of the carbonyl group. The electron density and its distance to the lysine amino group indicated that, in the conditions used for crystallization, no covalent bond was formed between the inhibitor and the enzyme active site. The C2−C3 region of the inhibitor formed an aromatic stacking interaction with

Scheme 3. Synthesis of Pyrrolo[2,3-*a*]carbazole Derivatives Substituted at the C-7 Position[a]

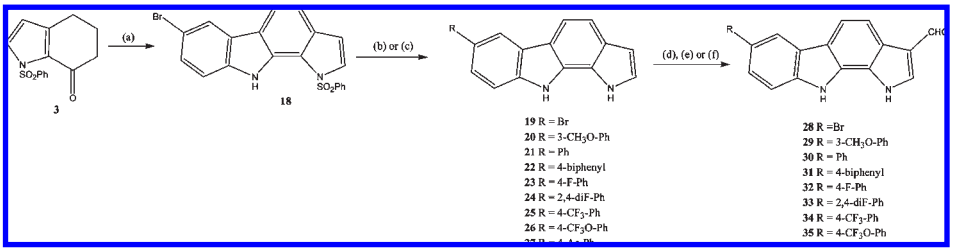

[a] Reagents and conditions. (a) (i) 4-Br-PhNHNH$_2$, choline chloride-ZnCl$_2$ 1:2, 120 °C, (ii) DDQ, dioxane, 74%; (b) NaOH, MeOH, 92%; (c) (i) ArB(OH)$_2$, Pd(PPh$_3$)$_2$Cl$_2$, aq Na$_2$CO$_3$, THF, (ii) aq NaOH, 50−65%; (d) (i) (COCl)$_2$, DMF, CH$_2$Cl$_2$, 0 °C, (ii) aq NaOH, rt, R = Br, 66%; (e) (i) POCl$_3$, DMF, 120 °C, (ii) aq NaOH, rt, R = 3-CH$_3$O-Ph, 45%; (f) (i) POCl$_3$, DMF, 100 °C, μw, (ii) aq NaOH, 30−67%.

Table 3. In Vitro Antiproliferative Activity (IC_{50} in μM) of Compounds **9** and **28**

	IC_{50} (μM)			
compd	PC3	DU145	PA1	fibroblast
9	9.5 ± 0.5	26 ± 2	4.5 ± 0.4	21 ± 1
28	5.9 ± 0.4	12.2 ± 0.8	2.8 ± 0.2	11 ± 1

Table 4. Data Collection and Refinement of the Pim-1 Crystal Structure in Complex with Compound **9**

Data Collection	
PDB ID	3JPV
space group	$P6_5$
cell dimensions: *a*, *b*, *c* (Å)	97.82 97.82 80.74
resolution[a] (Å)	2.35 (2.48−2.35)
unique observations[a]	18386 (2654)
completeness[a] (%)	99.9 (100.0)
redundancy[a]	4.6 (4.6)
R_{merge}[a]	0.127 (0.763)
$I/\sigma I$[a]	10.6 (2.0)
Refinement	
resolution (Å)	2.35
R_{work}/R_{free} (%)	17.5/23.1
no. of atoms (protein/other/water)	2213/83/160
B factors (Å^2) (protein/other/water)	22.03/29.59/30.63
rmsd bonds (Å)	0.015
rmsd angles (deg)	1.540
Ramachadran:	
favored (%)	91.5
allowed (%)	7.6
generously allowed (%)	0.8
disallowed (%)	0.0

[a] Values in parentheses correspond to the highest resolution shell.

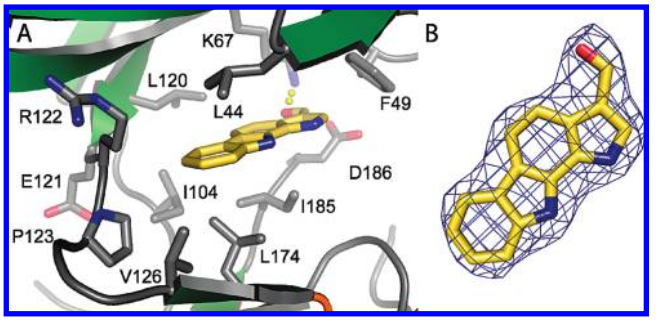

Figure 2. Binding of compound **9** to the ATP binding site of Pim-1. (A) Residues in the vicinity of the inhibitor are shown in stick representation and are labeled. Carbon atoms of the inhibitor are shown in yellow and carbon atoms of the substrate peptide are colored in white. (B) $2F_oF_c$ electron density map around the inhibitor contoured at 2σ.

the P-loop phenylalanine Phe49, which is flipped into the kinase active site as observed in a number of other Pim-1 inhibitor complexes.[42−45]

The presence of a proline residue in the Pim hinge region does not permit the formation of two hydrogen bonds to ATP or ATP mimetic inhibitors. However, a number of inhibitors including flavonoid and bisindolylmaleimide showed typical ATP mimetic hinge binding when crystallized with Pim-1.[29,42] The structure of an imidazo[1,2-*b*]pyridazine showed recently that this inhibitor class interacts with Pim-1 in a non-ATP mimetic binding mode.[23] In this structure, the inhibitor formed similar interactions with Pim-1 as observed for compound **9**, including polar interaction with lysine 67, aromatic interactions with the glycine rich loop residue Phe49, and a number of hydrophobic contacts involving Leu44, Ile104, and Leu120. Thus, it seems that for Pim kinase inhibitors can be efficiently anchored by polar contacts with the active site lysine and by hydrophobic interaction to Pim active site residues.

Key residues interacting with compound **9** are conserved within Pim family members. It is therefore surprising that compound **9** and a number of similar compounds show selectivity for Pim-1 and Pim-3 over Pim-2. Preferential binding of inhibitors to Pim-1 over Pim-2 has been noted before.[23,42] Comparing the structures of Pim-1 with Pim-2 (PDB code 2IWI) revealed that only four residues are different between the two active sites. Interestingly two residues are located in the hinge region substituting the Pim-1 residue Glu124 with a leucine and Val126 with an alanine in Pim-2. The lack of polar interactions of Glu124 with Arg122 results most likely in the observed disorder of the arginine side chain in the Pim-2 crystal structure. Probably the destabilization of the hinge region in Pim-2 caused by the Glu124Leu substitution influence hinge dynamics and consequently inhibitor binding. Also the Val126/Ala substitution in Pim-2 may result in slighly reduced hydrophobic interactions with the inhibitor. In addition, substitutions in the glycine rich loop residues located in a region that hinges the movement of Phe49 into the active site (Ser51Thr; Ser46Lys) may influence the energy barrier of this movement and may result in weaker inhibitor binding for Pim-2. However, more detailed studies are necessary to unravel differences of dynamic active site properties of Pim family members.

Conclusion

In conclusion, this work reports a structure−activity relationship studies of new pyrrolo[2,3-*a*]carbazoles as Pim kinase

inhibitors. An improved synthesis of the pyrrolo[2,3-*a*]-carbazole scaffold by Fischer indole synthesis in ionic liquid conditions was achieved to get an easier access to diversely substituted derivatives. Compound **9**, substituted at the C-3 position by a formyl group, exhibited a potent and selective inhibitory potency of Pim kinases when tested toward a panel of 66 kinases, with a higher activity against Pim-3 kinase in the nanomolar range. In addition, compound **9** and its C-7 brominated analogue **28** were evaluated for their in vitro antiproliferative potencies toward three cancer cell lines and a fibroblast primary culture. IC_{50} values in the micromolar range were determined for compounds **9** and **28** toward PA1 and PC3 cell lines. Finally, the structure of a cocrystal **9**/Pim-1 was resolved by X-ray analysis, showing the interaction of **9** within the ATP binding site. This X-ray structure provided valuable information that will facilitate further development of the structure based design of new Pim kinase inhibitors in this series, work that has already been initiated in our laboratory.

Experimental Section

Chemistry. General. IR spectra were recorded on a Perkin-Elmer Paragon 500 spectrometer ($\bar{\nu}$ in cm^{-1}). NMR spectra were performed on a Bruker AVANCE 400 (^1H, 400 MHz; ^{13}C, 100 MHz) or AVANCE 500 (^1H, 500 MHz; ^{13}C, 125 MHz), chemical shifts δ in ppm, the following abbreviations are used: singlet (s), doublet (d), broad doublet (br d), triplet (t), quadruplet (q), doublet of doublet (dd), doublet of doublet of doublet (ddd), sextuplet (sx), multiplet (m), broad signal (br s). Mass spectra (ESI+) were determined on a high-resolution Micro Q-Tof apparatus. Mass spectra (FAB+) were determined on a high-resolution Fisons Autospec-Q spectrometer at CESAMO (Talence, France). Chromatographic purifications were performed by flash silica gel Geduran SI 60 (Merck) 0.040−0.063 mm column chromatography. Reactions were monitored by TLC using fluorescent silica gel plates (60 F254 from Merck). Experiments under microwave irradiation were performed using a CEM Discover Benchmate apparatus. Melting points were measured on a Reichert microscope and are uncorrected. The purity of tested compounds was established to be ≥95% by HPLC analysis using a Dionex liquid chromatograph (TCC-100, 25 °C; P580; UVD340U) and a C18 Dionex Acclaim 120 column (4.6 mm × 250 mm, 5 μm, 120 Å). Detection wavelength is indicated for each compound. Solvents were (A) water, 0.1% TFA; (B) acetonitrile; (C) water; system I: 95:5 A/B for 5 min and then 95:5 A/B to 5:95 A/B in 30 min and then 5:95 A/B for 5 min; 0.8 mL/min; system II: 95:5 C/B for 5 min and then 95:5 C/B to 5:95 C/B in 30 min and then 5:95 C/B for 5 min; 0.8 mL/min.

3-Benzenesulfonyl-3,10-dihydropyrrolo[3,2-*a*]carbazole (4). Phenylhydrazine (1.73 mL, 17.6 mmol) was added to a solution of **2** (2.42 g, 8.8 mmol) in glacial acetic acid (35 mL). The mixture was refluxed for 38 h. After evaporation, the residue was purified by flash chromatography (cyclohexane/EtOAc, from 99:1 to 8:2) to give **4** (740 mg, 2.14 mmol, 24%) as a light-yellow solid; mp 185 °C. HRMS (ESI+) calcd for $C_{20}H_{15}N_2O_2S$ $(M + H)^+$ 347.0854, found 347.0855. IR (KBr): 3420 cm^{-1}. ^1H NMR (400 MHz, DMSO-d_6): 7.21 (1H, d, J = 4.0 Hz), 7.22 (1H, t, J = 7.5 Hz), 7.40 (1H, t, J = 7.5 Hz), 7.58 (1H, d, J = 8.0 Hz), 7.61 (2H, t, J = 8.0 Hz), 7.70 (1H, t, J = 7.5 Hz), 7.82 (1H, d, J = 8.5 Hz), 7.88 (1H, d, J = 3.5 Hz), 8.03 (2H, d, J = 7.5 Hz), 8.10 (1H, d, J = 8.5 Hz), 8.13 (1H, d, J = 8.0 Hz), 11.84 (1H, s, NH). ^{13}C NMR (100 MHz, DMSO-d_6): 104.7, 107.0, 111.1, 117.3, 119.0, 119.7, 124.6, 125.5, 126.6 (2C), 129.7 (2C), 134.5 (CH), 115.5, 117.3, 122.8, 132.6, 133.0, 137.1, 139.0 (C).

3,10-Dihydropyrrolo[3,2-*a*]carbazole (5). A 5 M aq NaOH solution (18 mL) was added to a solution of **4** (738 mg, 2.13 mmol) in MeOH (180 mL). The mixture was refluxed for 15 h, and methanol was evaporated. Water was added, and the mixture was extracted with EtOAc. The organic fractions were washed with saturated aq $NaHCO_3$, brine, and dried over $MgSO_4$. After evaporation, the residue was purified by flash chromatography (cyclohexane/EtOAc, from 95:5 to 8:2) to give **5** (420 mg, 2.04 mmol, 96%) as a yellow solid. HPLC purity, system I: >99%, λ = 248 nm, t_R = 23.8 min. For spectral data of compound **5**, see ref 33.

1-Benzenesulfonyl-1,10-dihydropyrrolo[2,3-*a*]carbazole (6). Preparation of the Ionic Liquid. A mixture of choline chloride (10.0 g, 71.6 mmol) and zinc chloride (19.5 g, 143 mmol) in toluene (200 mL) was refluxed in a Dean−Stark apparatus under vigorous stirring for 15 h. After cooling and decantation, the ionic liquid was obtained as a yellow oil, which can be directly used or conserved under inert atmosphere in anhyd ether.

Step A. A mixture of phenylhydrazine (393 mg, 3.63 mmol), **3** (500 mg, 1.82 mmol), and ionic liquid (5.25 g, 12.7 mmol) was stirred at 120 °C for 2 h. After cooling, a 0.5 M aq HCl solution was added before extraction with EtOAc (3 × 50 mL). The organic fractions were washed with brine and then dried over $MgSO_4$. The solution contained the major indolization product and the minor expected product.

Step B. DDQ (0.29 g, 1.28 mmol, necessary DDQ quantity was determined from a ^1H NMR spectrum of the intermediate mixture) was added to this solution and the mixture was stirred at room temperature for 15 h. The mixture was washed with brine and dried over $MgSO_4$. After evaporation, the residue was purified by flash chromatography (pentane/EtOAc, 95:5 then 90:10) to give **6** (490 mg, 1.41 mmol, 78% yield) as a white solid; mp 148 °C. HRMS (ESI+) calcd for $C_{20}H_{15}N_2O_2S$ $(M + H)^+$ 347.0854, found 347.0861. IR (KBr): 3430, 1630, 1610 cm^{-1}. ^1H NMR (400 MHz, DMSO-d_6): 6.85 (1H, d, J = 3.5 Hz), 7.28−7.39 (4H, m), 7.44−7.52 (2H, m), 7.53 (1H, d, J = 3.5 Hz), 7.64 (1H, d, J = 8.0 Hz), 7.75−7.80 (2H, m), 8.01 (1H, d, J = 8.0 Hz), 8.12 (1H, d, J = 8.0 Hz), 10.12 (1H, br s, NH). ^{13}C NMR (100 MHz, DMSO-d_6): 111.4, 112.6, 113.0, 117.1, 119.9 (2C), 125.5, 126.1, 126.7 (2C), 129.5 (2C), 133.9 (CH), 120.4, 121.9, 123.8, 127.0, 130.6, 137.9, 138.8 (C). HPLC purity, system I: >99%, λ = 306 nm, t_R = 28.6 min.

1,10-Dihydropyrrolo[2,3-*a*]carbazole (7). A 5 M aq NaOH solution (125 mL) was added to a suspension of **6** (3.12 g, 9.0 mmol) in MeOH (1.0 L). The mixture was refluxed for 12 h. The reaction mixture was then concentrated under vacuum until formation of a precipitate, which was collected by filtration. The solid was washed with MeOH (10 mL) and then with Et_2O (2 × 30 mL) to give **7** (1.71 g, 8.3 mmol, 92%) as an off-white powder; mp 295 °C. HRMS (ESI+) calcd for $C_{14}H_{11}N_2$ $(M + H)^+$ 207.0922, found 207.0925. IR (KBr): 3420, 3385, 1650, 1455, 1445, 1395, 1345, 1310 cm^{-1}. ^1H NMR (400 MHz, DMSO-d_6): 6.61 (1H, dd, J_1 = 3.0 Hz, J_2 = 2.0 Hz), 7.18 (1H, ddd, J_1 = 8.0 Hz, J_2 = 7.0 Hz, J_3 = 1.0 Hz), 7.33 (1H, ddd, J_1 = 8.0 Hz, J_2 = 7.0 Hz, J_3 = 1.0 Hz), 7.37 (1H, d, J = 8.5 Hz), 7.42 (1H, t, J = 3.0 Hz), 7.64 (1H, d, J = 8.0 Hz), 7.75 (1H, d, J = 8.5 Hz), 8.07 (1H, d, J = 7.5 Hz), 10.88 (1H, br s, NH), 10.95 (1H, br s, NH). ^{13}C NMR (100 MHz, DMSO-d_6): 102.8, 111.2, 112.0, 112.1, 118.6, 119.0, 123.3, 123.6 (CH), 116.2, 121.8, 124.1, 126.2, 126.4, 138.1 (C). HPLC purity, system I: >99%, λ = 249 nm, t_R = 24.5 min.

3,10-Dihydropyrrolo[3,2-*a*]carbazole-1-carbaldehyde (8). A solution of oxalyl chloride (89 μL, 1.02 mmol) and DMF (86 μL, 1.11 mmol) in CH_2Cl_2 (25 mL) was stirred at 0 °C for 20 min. A solution of **5** (200 mg, 0.97 mmol) in anhyd CH_2Cl_2 (25 mL) was then added dropwise. The mixture was stirred at 0 °C for 20 min and then for 2.5 h at room temperature. After evaporation, 5% aq NaOH solution (50 mL) was added. The mixture was stirred overnight and water was added. The mixture was extracted with EtOAc and the organic fractions were dried over $MgSO_4$. After evaporation, the residue was purified by flash chromatography (cyclohexane/EtOAc, from 7:3 to 5:5) to give **8** (151 mg, 0.645 mmol, 66%) as a white solid; mp 218−220 °C. HRMS (FAB+) calcd for $C_{15}H_{10}N_2O$ $(M)^+$ 234.0793, found

234.0791. IR (KBr): 3400, 3300−3150, 1625 cm^{-1}. ^1H NMR (400 MHz, DMSO-d_6): 7.22 (1H, ddd, J_1 = 8.0 Hz, J_2 = 7.0 Hz, J_3 = 1.0 Hz), 7.37 (1H, d, J = 8.5 Hz), 7.38 (1H, ddd, J_1 = 8.0 Hz, J_2 = 7.0 Hz, J_3 = 1.0 Hz), 7.86 (1H, d, J = 8.0 Hz), 8.05 (1H, d, J = 8.5 Hz), 8.13 (1H, d, J = 8.0 Hz), 8.41 (1H, s), 10.0 (1H, s, CHO), 10.70 (1H, s), 12.50 (1H, s). ^{13}C NMR (100 MHz, DMSO-d_6): 104.5, 112.0, 116.5, 118.8, 119.0, 123.9, 136.7 (CH), 109.2, 116.1, 118.8, 123.3, 132.7, 136.0, 137.8 (C), 185.3 (C═O). HPLC purity, system I: >99%, λ = 241 nm, t_R = 23.3 min.

1,10-Dihydropyrrolo[2,3-*a*]carbazole-3-carbaldehyde (9). A solution of oxalyl chloride (19.5 μL, 0.224 mmol) and DMF (19 μL, 0.245 mmol) in anhyd CH_2Cl_2 (6 mL) was stirred at 0 °C for 20 min. A solution of **7** (43.6 mg, 0.211 mmol) in anhyd CH_2Cl_2 (6 mL) was then added dropwise. The solution was stirred at 0 °C for 20 min then for 2.5 h at room temperature. After evaporation, 5% aq NaOH (12 mL) was added. The mixture was stirred for 12 h. After addition of water, the mixture was extracted with EtOAc and the organic fractions were dried over $MgSO_4$. After evaporation, the residue was purified by flash chromatography (cyclohexane/EtOAc, from 7:3 to 5:5) to give **9** (32.4 mg, 0.138 mmol, 65%) as a white solid; mp > 290 °C. HRMS (ESI+) calcd for $C_{15}H_{11}N_2O$ $(M + H)^+$ 235.0871, found 235.0882. IR (KBr): 3450−3150, 1630, 1615 cm^{-1}. ^1H NMR (500 MHz, DMSO-d_6): 7.23 (1H, t, J = 7.5 Hz), 7.40 (1H, t, J = 7.5 Hz), 7.70 (1H, d, J = 8.0 Hz), 7.96 (1H, d, J = 8.5 Hz), 8.00 (1H, d, J = 8.5 Hz), 8.15 (1H, d, J = 7.5 Hz), 8.33 (1H, d, J = 2.0 Hz), 10.07 (1H, s), 11.10 (1H, br s), 11.93 (1H, br s). ^{13}C NMR (125 MHz, DMSO-d_6): 111.5, 112.1, 115.0, 119.0, 119.5, 124.3, 136.7 (CH), 118.3, 119.5, 122.5, 122.8, 123.5, 126.0, 138.5 (C), 185.3 (C═O). HPLC purity, system I: >99%, λ = 247 nm, t_R = 21.7 min.

(1,10-Dihydropyrrolo[2,3-*a*]carbazol-3-yl)methanol (10). $NaBH_4$ (320 mg, 8.46 mmol) was added to a solution of **9** (147 mg, 0.63 mmol) in MeOH (30 mL), and the mixture was stirred at room temperature for 1 h. H_2O (10 mL) was added, and the precipitate was collected by filtration. The solid was washed with MeOH (5 mL) and then with Et_2O (2 × 20 mL) to give **10** (100 mg, 0.423 mmol, 67%) as a gray powder; mp > 295 °C. HRMS (ESI+) calcd for $C_{15}H_{11}N_2$ $(M - OH)^+$ 219.0922, found 219.0922. IR (KBr): 3375, 1648, 1456 cm^{-1}. ^1H NMR (400 MHz, DMSO-d_6): 4.72 (2H, s), 4.54−4.96 (1H, br s), 7.14 (1H, t, J = 7.5 Hz), 7.26−7.31 (2H, m), 7.40 (1H, d, J = 8.5 Hz), 7.58 (1H, d, J = 8.0 Hz), 7.71 (1H, d, J = 8.5 Hz), 8.03 (1H, d, J = 7.5 Hz), 10.48−11.46 (2H, 2 br s). ^{13}C NMR (100 MHz, DMSO-d_6): 55.7 (CH_2), 110.9, 111.1, 111.5, 118.5, 119.0, 121.8, 123.3 (CH), 116.3, 117.7, 122.1, 124.1, 125.1, 126.4, 138.1 (C). HPLC purity, system II: >97%, λ = 252 nm, t_R = 20.6 min.

1,10-Dihydropyrrolo[2,3-*a*]carbazole-3-carboxamide (11). Chlorosulfonylisocyanate (27 μL, 0.31 mmol) was added at 0 °C to a solution of **7** (57.4 mg, 0.278 mmol) in anhyd acetonitrile (10 mL). The mixture was stirred at 0 °C for 1.5 h, and a 1N aq hydrogen chloride solution (5 mL) and THF (2 mL) were added. The mixture was stirred at room temperature for 36 h, and water was added. After extraction with EtOAc, the combined organic fractions were washed with an aq saturated $NaHCO_3$ solution, brine, dried over $MgSO_4$, and evaporated. The residue was purified by flash chromatography (eluent: THF) to give **11** (13.8 mg, 0.055 mmol, 20%) as a beige solid; mp > 300 °C. HRMS (ESI+) calcd for $C_{15}H_{12}N_3O$ $(M + H)^+$ 250.0980, found 250.0966. IR (KBr): 3430, 3370, 3335, 1650 cm^{-1}. ^1H NMR (500 MHz, DMSO-d_6): 6.86 (1H, br s), 7.20 (1H, t, J = 8.0 Hz), 7.36 (1H, ddd, J_1 = 8.0 Hz, J_2 = 7.0 Hz, J_3 = 1.0 Hz), 7.46 (1H, br s), 7.65 (1H, d, J = 8.0 Hz), 7.84 (1H, d, J = 8.5 Hz), 8.02 (1H, d, J = 8.5 Hz), 8.08 (1H, d, J = 3.0 Hz), 8.10 (1H, d, J = 8.0 Hz). ^{13}C NMR (100 MHz, DMSO-d_6): 111.3, 112.8, 113.2, 118.7, 119.2, 123.7, 126.8 (CH), 112.1, 116.8, 112.1, 123.8, 124.8, 126.2, 138.3 (C), 166.7 (C═O). HPLC purity, system I: >99%, λ = 248 nm, t_R = 19.2 min.

1-(1,10-Dihydropyrrolo[2,3-*a*]carbazol-3-yl)-2,2,2-trifluoroethanone (12). Trifluoroacetic anhydride (45 μL, 0.32 mmol) was added at room temperature to a solution of **7** (52 mg, 0.25 mmol) in DMF (10 mL). The mixture was stirred at room temperature for 18 h and ice and then water (10 mL) were added. The aqueous layer was extracted with EtOAc (3 × 10 mL). The organic fractions were combined, washed with brine (15 mL), dried over $MgSO_4$, and evaporated. The residue was triturated in Et_2O (20 mL) and the mixture was filtered to give **12** (32 mg, 0.106 mmol, 42%) as a green powder; mp > 295 °C. HRMS (ESI+) calcd for $C_{16}H_{10}F_3N_2O$ $(M + H)^+$ 303.0745, found 303.0732. IR (KBr): 3274, 1639 cm^{-1}. ^1H NMR (400 MHz, DMSO-d_6): 7.22 (1H, t, J = 7.5 Hz), 7.40 (1H, ddd, J_1 = 8.0 Hz, J_2 = 7.0 Hz, J_3 = 1.0 Hz), 7.70 (1H, d, J = 8.0 Hz), 8.01 (1H, d, J = 8.5 Hz), 8.07 (1H, d, J = 8.5 Hz), 8.15 (1H, d, J = 8.0 Hz), 8.49−8.53 (1H, br s), 11.03 (1H, s), 12.39−12.48 (1H, br s). ^{13}C NMR (100 MHz, DMSO-d_6): 111.7, 112.1, 116.3, 119.3, 119.7, 124.7, 135.8 (q, J_{CF} = 5 Hz) (CH), 110.1, 117.0 (q, J_{CF} = 292 Hz), 119.1, 122.3, 123.2, 124.1, 126.0, 138.6 (C), 174.0 (q, J_{CF} = 34 Hz, C═O). HPLC purity, system I: >98%, λ = 245 nm, t_R = 25.6 min.

Ethyl 2-(1,10-Dihydropyrrolo[2,3-*a*]carbazol-3-yl)-2-oxoacetate (14). Step A. Oxalyl chloride (660 μL, 7.7 mmol) was added to a suspension of **7** (825 mg, 4.00 mmol) in anhyd Et_2O (40 mL) at 0 °C. The mixture was stirred at room temperature for 4 h. After filtration, the solid was washed with Et_2O (2 × 40 mL) to give the acid chloride intermediate **13** (972 mg) as a red−brown solid, which was used without further purification.

Step B. Triethylamine (275 μL, 1.97 mmol) was added to a suspension of the acid chloride intermediate (486 mg) in EtOH (10 mL). The mixture was stirred at room temperature for 4 h. After filtration, the solid was washed with EtOH (10 mL) and then with Et_2O (2 × 20 mL) to give **14** (446 mg, 1.46 mmol, 73% from **7**) as a yellow−green powder; mp > 295 °C. HRMS (ESI+) calcd for $C_{18}H_{14}N_2NaO_3$ $(M + Na)^+$ 329.0902, found 329.0907. IR (KBr): 3292, 1725, 1602 cm^{-1}. ^1H NMR (400 MHz, DMSO-d_6): 1.37 (3H, t, J = 7.0 Hz), 4.39 (2H, q, J = 7.0 Hz), 7.20 (1H, t, J = 7.5 Hz), 7.38 (1H, ddd, J_1 = 8.0 Hz, J_2 = 7.0 Hz, J_3 = 1.0 Hz), 7.67 (1H, d, J = 8.0 Hz), 7.98−8.03 (2H, m), 8.12 (1H, d, J = 8.0 Hz), 8.47 (1H, d, J = 3.0 Hz), 11.07 (1H, s), 12.09−12.20 (1H, br s). ^{13}C NMR (100 MHz, DMSO-d_6): 14.0 (CH_3), 61.6 (CH_2), 111.6, 112.3, 115.7, 119.1, 119.6, 124.5, 136.6 (CH), 113.7, 118.7, 122.4, 123.3, 123.8, 126.1, 138.5 (C), 163.7, 179.4 (C═O).

2-(1,10-Dihydropyrrolo[2,3-*a*]carbazol-3-yl)-*N*,*N*-diethyl-2-oxoacetamide (15). The acid chloride intermediate **13** was prepared as described above for the preparation of compound **14**. Diethylamine (305 μL, 2.92 mmol) was added to a suspension of the acid chloride intermediate (486 mg) in anhyd diethylether (10 mL). The mixture was stirred at room temperature for 4 h. After filtration, the solid was washed with MeOH (3 mL) and then with Et_2O (2 × 20 mL) to give **15** (439 mg, 1.32 mmol, 66% from **7**) as a pale-gray powder; mp > 295 °C. HRMS (ESI+) calcd for $C_{20}H_{20}N_3O_2$ $(M + H)^+$ 334.1556, found 334.1543. IR (KBr): 3450−3100, 1635, 1608, 1429 cm^{-1}. ^1H NMR (400 MHz, DMSO-d_6): 1.10 (3H, t, J = 7.0 Hz), 1.22 (3H, t, J = 7.0 Hz), 3.28 (2H, q, J = 7.0 Hz), 3.47 (2H, q, J = 7.0 Hz), 7.20 (1H, ddd, J_1 = 8.0 Hz, J_2 = 7.0 Hz, J_3 = 1.0 Hz), 7.37 (1H, ddd, J_1 = 8.0 Hz, J_2 = 7.0 Hz, J_3 = 1.5 Hz), 7.66 (1H, d, J = 8.0 Hz), 7.93 (1H, d, J = 8.5 Hz), 7.99 (1H, d, J = 8.5 Hz), 8.07 (1H, d, J = 3.0 Hz), 8.12 (1H, d, J = 8.0 Hz), 11.04 (1H, s, NH), 11.96−12.01 (1H, br s, NH). ^{13}C NMR (100 MHz, DMSO-d_6): 12.7, 14.1 (CH_3), 38.1, 41.7 (CH_2), 111.4, 112.1, 115.3, 119.0, 119.5, 124.4, 134.9 (CH), 114.3, 118.3, 122.7, 123.2, 123.4, 126.1, 138.4 (C), 167.2, 187.0 (C═O).

2-(1,10-Dihydropyrrolo[2,3-*a*]carbazol-3-yl)ethanol (16). $LiAlH_4$ (2.00 mL, 2.00 mmol, 1 M in THF) was added at room temperature to a suspension of **14** (153 mg, 0.50 mmol) in dioxane (10 mL). THF was distilled, and the mixture was refluxed for 12 h. After cooling, water was added (5 mL) and

the mixture was extracted with EtOAc (3 × 10 mL). The organic fractions were combined, washed with H_2O (10 mL), dried over $MgSO_4$, and evaporated. The residue was triturated in Et_2O (20 mL) and filtered to give **16** (90 mg, 0.36 mmol, 72%) as a brown−gray powder; mp 269−271 °C. HRMS (ESI+) calcd for $C_{16}H_{15}N_2O$ $(M + H)^+$ 251.1184, found 251.1177. IR (KBr): 3416, 3382, 3234, 1649, 1457 cm^{-1}. ^1H NMR (400 MHz, DMSO-d_6): 2.92 (2H, t, J = 7.5 Hz), 3.71 (2H, dt, J_1 = 7.5 Hz, J_2 = 5.5 Hz), 4.63 (1H, t, J = 5.5 Hz), 7.13 (1H, ddd, J_1 = 8.0 Hz, J_2 = 7.0 Hz, J_3 = 1.0 Hz), 7.19 (1H, d, J = 2.0 Hz), 7.28 (1H, ddd, J_1 = 8.0, J_2 = 7.0 Hz, J_3 = 1.0 Hz), 7.31 (1H, d, J = 8.5 Hz), 7.58 (1H, d, J = 8.0 Hz), 7.70 (1H, d, J = 8.5 Hz), 8.02 (1H, d, J = 7.5 Hz), 10.53−10.57 (1H, br s), 10.86 (1H, s). ^{13}C NMR (100 MHz, DMSO-d_6): 29.1, 61.8 (CH_2), 110.4, 111.1, 111.3, 118.5, 119.0, 121.2, 123.2 (CH), 113.3, 116.2, 121.9, 124.1, 125.9, 126.5, 138.1 (C). HPLC purity, system I: >98%, λ = 252 nm, t_R = 21.4 min.

2-(1,10-Dihydropyrrolo[2,3-*a*]carbazol-3-yl)-*N*,*N*-diethyl-2-hydroxyiminoethanamide (17). Hydroxylamine hydrochloride (261 mg, 3.76 mmol) was added to a solution of **16** (167 mg, 0.50 mmol) in pyridine (5 mL) and the mixture was refluxed for 12 h. H_2O (5 mL) was added, and pyridine was removed under vacuum. The aqueous layer was extracted with EtOAc (3 × 10 mL), and the combined organic fractions were washed with brine (10 mL), dried over $MgSO_4$, and evaporated. The residue was triturated in EtOAc (20 mL) and filtered to give **17** (33 mg, 0.095 mmol, 19%) as a pale-beige powder; mp 268−269 °C. HRMS (ESI+) calcd for $C_{20}H_{21}N_4O_2$ $(M + H)^+$ 349.1665, found 349.1675. IR (KBr): 3266, 1609 cm^{-1}. ^1H NMR (400 MHz, DMSO-d_6): 1.03 (3H, t, J = 7.0 Hz), 1.19 (3H, t, J = 7.0 Hz), 3.26 (2H, q, J = 7.0 Hz), 3.39−3.59 (2H, m), 7.17 (1H, t, J = 7.5 Hz), 7.33 (1H, t, J = 7.5 Hz), 7.36 (1H, d, J = 2.5 Hz), 7.61 (1H, d, J = 8.0 Hz), 7.83 (1H, d, J = 8.5 Hz), 7.86 (1H, d, J = 8.5 Hz), 8.07 (1H, d, J = 7.5 Hz), 10.90 (1H, s), 11.03−11.07 (1H, br s), 11.21−11.26 (1H, br s). ^{13}C NMR (100 MHz, DMSO-d_6): 12.8, 13.8 (CH_3), 37.6, 41.7 (CH_2), 111.3, 113.2, 113.3, 118.7, 119.3, 123.8, 125.7 (CH), 109.7, 117.3, 122.5, 122.7, 123.7, 126.2, 138.3 (C), 150.6 (C═N), 164.4 (C═O). HPLC purity, system I: >99%, λ = 251 nm, t_R = 21.5 min.

1-Benzenesulfonyl-7-bromo-1,10-dihydropyrrolo[2,3-*a*]carbazole (18). Step A. A suspension of 4-bromophenylhydrazine hydrochloride (1.62 g, 7.3 mmol) and anhyd sodium acetate (0.60 g, 7.3 mmol) in DME (20 mL) was stirred at room temperature for 1 h. Compound **3** (1.00 g, 3.63 mmol) and ionic liquid (10.0 g, 24.3 mmol, prepared as for the synthesis of compound **6**) were added. The solvent was evaporated, and the mixture was stirred at 120 °C for 2 h. After cooling, a 0.5 M aq HCl solution was added before extraction with EtOAc. The organic fractions were washed with brine, dried over $MgSO_4$, and evaporated. The residue contained the major indolization product and the minor expected product.

Step B. A solution of the residue from step A and DDQ (0.7 g, 3.1 mmol, necessary DDQ quantity was determined from a ^1H NMR spectrum of the intermediate mixture) in dioxane (20 mL) was stirred at room temperature for 15 h. After evaporation, EtOAc was added and the mixture was washed with water, with brine, dried over $MgSO_4$, and evaporated. The residue was purified by flash chromatography (pentane/EtOAc 9:1) to give **18** (1.15 g, 2.70 mmol, 74%) as a brown solid; mp 173−175 °C. IR (KBr): 3434, 1631 cm^{-1}. HRMS (ESI+) calcd for $C_{20}H_{14}{}^{79}BrN_2O_2S$ $(M + H)^+$ 424.9959, found 424.9976. ^1H NMR (400 MHz, DMSO-d_6): 7.04 (1H, d, J = 3.5 Hz), 7.41 (1H, d, J = 8.0 Hz), 7.49−7.55 (3H, m), 7.62 (1H, t, J = 7.5 Hz), 7.84 (1H, d, J = 3.5 Hz), 7.92−7.99 (3H, m), 8.12 (1H, d, J = 8.0 Hz), 8.38 (1H, d, J = 1.5 Hz), 10.81 (1H, s, NH). ^{13}C NMR (100 MHz, DMSO-d_6): 112.4, 113.2, 114.9, 117.4, 121.9, 126.7 (2C), 127.0, 127.5, 129.9 (2C), 134.6 (CH), 111.7, 119.4, 120.1, 124.7, 126.6, 130.8, 136.8, 137.7 (C).

7-Bromo-1,10-dihydropyrrolo[2,3-*a*]carbazole (19). A 5 M aq NaOH solution (10 mL) was added to a suspension of **18** (500 mg, 1.18 mmol) in methanol (100 mL). The mixture was refluxed for 12 h. The reaction mixture was then concentrated under vacuum until there was formation of a precipitate. The mixture was neutralized by addition of concentrated HCl, and the solid was filtered off and washed with water to give **19** (310 mg, 1.09 mmol, 92%) as a brown solid; mp 250 °C (decomposition). HRMS (ESI+) calcd for $C_{14}H_{10}{}^{79}BrN_2$ $(M + H)^+$ 285.0027, found 285.0040. IR (KBr): 3400, 1648, 1438 cm^{-1}. ^1H NMR (400 MHz, DMSO-d_6): 6.59 (1H, dd, J_1 = 3.0 Hz, J_2 = 2.0 Hz), 7.35 (1H, d, J = 8.5 Hz), 7.38−7.42 (2H, m), 7.58 (1H, d, J = 8.5 Hz), 7.74 (1H, d, J = 8.5 Hz), 8.25 (1H, d, J = 2.0 Hz), 10.88−10.92 (1H, br s, NH), 11.05−11.09 (1H, br s, NH). ^{13}C NMR (100 MHz, DMSO-d_6): 102.9, 112.2, 112.6, 113.1, 121.5, 124.0, 125.6 (CH), 110.8, 115.3, 121.5, 126.1, 126.7, 127.1, 136.8 (C).

General Procedure for the Preparation of Compounds (20−27). To a solution of **18** (425 mg, 1 mmol) in THF (5 mL) were added a solution of sodium carbonate (212 mg, 2 mmol) in water (1 mL), $Pd(PPh_3)_2Cl_2$ (35.1 mg, 0,05 mmol) and the corresponding boronic acid (1.1 equiv). The mixture was refluxed overnight. After cooling, the mixture was filtered on celite and the solid was washed with acetone. After evaporation of the filtrate, methanol (40 mL) and a 5 M aq NaOH solution (20 mL) were added and the mixture was refluxed for 12 h. After concentration under vacuum and neutralization with concentrated HCl, EtOAc was added. The organic layer was collected, and the aqueous phase was extracted with EtOAc (3 × 30 mL). The combined organic phases were washed with brine, dried over $MgSO_4$, and evaporated. The residue was purified by flash chromatography (pentane/EtOAc, from 9:1 to 7:3) to give the attempted compound.

7-(3-Methoxyphenyl)-1,10-dihydropyrrolo[2,3-*a*]carbazole (20). Compound **20** (172 mg, 0.55 mmol, 55%) as a brown solid; mp 202−205 °C. HRMS (ESI+) calcd for $C_{21}H_{17}N_2O$ $(M + H)^+$ 313.1341, found 313.1343. IR (KBr): 3390, 1654, 1609, 1584, 1461 cm^{-1}. ^1H NMR (400 MHz, DMSO-d_6): 3.86 (3H, s, CH_3), 6.59 (1H, dd, J_1 = 3.0 Hz, J_2 = 2.0 Hz), 6.90 (1H, ddd, J_1 = 8.0 Hz, J_2 = 2.5 Hz, J_3 = 1.5 Hz), 7.29−7.31 (1H, m), 7.34 (1H, dt, J_1 = 7.5 Hz, J_2 = 1.5 Hz), 7.36 (1H, d, J = 8.5 Hz), 7.39 (1H, t, J = 7.5 Hz), 7.39 (1H, t, J = 2.5 Hz), 7.61 (1H, dd, J_1 = 8.5 Hz, J_2 = 1.5 Hz), 7.67 (1H, d, J = 8.5 Hz), 7.82 (1H, d, J = 8.5 Hz), 8.36 (1H, d, J = 1.5 Hz), 10.83−10.88 (1H, br s, NH), 10.95−11.00 (1H, br s, NH). ^{13}C NMR (100 MHz, DMSO-d_6): 55.1 (CH_3), 102.8, 111.5, 111.8, 112.2 (3C), 117.3, 119.1, 122.6, 123.7, 129.8 (CH), 116.4, 121.8, 124.7, 126.4, 127.0, 131.0, 137.8, 143.2, 159.7 (C).

7-Phenyl-1,10-dihydropyrrolo[2,3-*a*]carbazole (21). Compound **21** (169 mg, 0.60 mmol, 60%) as a gray solid; mp > 250 °C. HRMS (ESI+) calcd for $C_{20}H_{15}N_2$ $(M + H)^+$ 283.1235, found 283.1248. IR (KBr): 3434, 3368, 1652 cm^{-1}. ^1H NMR (400 MHz, DMSO-d_6): 6.59 (1H, dd, J_1 = 3.0 Hz, J_2 = 2.0 Hz), 7.30−7.35 (1H, m), 7.37 (1H, J_1 = 8.5 Hz, J_2 = 0.5 Hz), 7.40 (1H, dd, J_1 = 3.0 Hz, J_2 = 2.5 Hz), 7.45−7.50 (2H, m), 7.61 (1H, dd, J_1 = 8.5 Hz, J_2 = 2.0 Hz), 7.68 (1H, dd, J_1 = 8.5 Hz, J_2 = 0.5 Hz), 7.76−7.79 (2H, m), 7.82 (1H, dd, J_1 = 8.5 Hz, J_2 = 0.5 Hz), 8.35 (1H, d, J = 2.0 Hz), 10.83−10.89 (1H, br s, NH), 10.96−11.00 (1H, br s, NH). ^{13}C NMR (100 MHz, DMSO-d_6): 102.9, 111.6, 112.2, 112.3, 117.2, 122.5, 123.7, 126.2, 126.7 (2C), 128.8 (2C) (CH), 116.4, 121.8, 124.8, 126.4, 127.0, 131.1, 137.8, 141.6 (C).

7-(4-Biphenyl)-1,10-dihydropyrrolo[2,3-*a*]carbazole (22). Compound **22** (230 mg, 0.64 mmol, 64%) as a brown solid; mp > 250 °C. HRMS (ESI+) calcd for $C_{26}H_{18}N_2$ $(M)^+$ 358.1470, found 358.1492. IR (KBr): 3650−3100, 1698, 1648 cm^{-1}. ^1H NMR (400 MHz, DMSO-d_6): 6.60 (1H, dd, J_1 = 3.0 Hz, J_2 = 2.0 Hz), 7.36−7.41 (3H, m), 7.47−7.52 (2H, m), 7.68 (1H, dd, J_1 = 8.5 Hz, J_2 = 1.5 Hz), 7.71 (1H, dd, J_1 = 8.5 Hz, J_2 = 0.5 Hz), 7.73−7.76 (2H, m), 7.77−7.80 (2H, m), 7.83 (1H, d, J = 8.5 Hz), 7.87−7.91 (2H, m), 8.41−8.43 (1H, m), 10.83−10.89 (1H, br s, NH), 10.98−11.02 (1H, br s, NH). ^{13}C NMR (100 MHz, DMSO-d_6): 102.8, 111.6, 112.2, 112.3, 117.1, 122.4, 123.7, 126.4 (2C), 127.0

(2C), 127.1 (2C), 127.3, 128.9 (2C) (CH), 116.4, 121.8, 124.8, 126.5, 127.0, 130.4, 137.8, 137.9, 139.8, 140.6 (C).

7-(4-Fluorophenyl)-1,10-dihydropyrrolo[2,3-*a*]carbazole (23). Compound **23** (150 mg, 0.50 mmol, 50%) as a gray−green solid; mp > 250 °C. HRMS (ESI+) calcd for $C_{20}H_{14}FN_2$ $(M + H)^+$ 301.1141, found 301.1154. IR (KBr): 3410, 3397, 1651, 1605, 1514 cm^{-1}. ^1H NMR (400 MHz, DMSO-d_6): 6.59 (1H, dd, J_1 = 3.0 Hz, J_2 = 2.0 Hz), 7.27−7.33 (2H, m), 7.36 (1H, d, J = 8.5 Hz), 7.39 (1H, dd, J_1 = 3.0 Hz, J_2 = 2.5 Hz), 7.58 (1H, dd, J_1 = 8.5 Hz, J_2 = 2.0 Hz), 7.68 (1H, dd, J_1 = 8.5 Hz, J_2 = 0.5 Hz), 7.77−7.83 (3H, m), 8.33 (1H, d, J = 2.0 Hz), 10.84−10.87 (1H, br s, NH), 10.96−10.98 (1H, br s, NH). ^{13}C NMR (100 MHz, DMSO-d_6): 102.8, 111.6, 112.2, 112.3, 115.5 (2C, d, J_{CF} = 21 Hz), 117.2, 122.4, 123.8, 128.5 (2C, d, J_{CF} = 8 Hz) (CH), 116.3, 121.8, 124.8, 126.5, 127.0, 130.1, 137.7, 138.1 (d, J_{CF} = 3 Hz), 161.2 (d, J_{CF} = 243 Hz) (C).

7-(2,4-Difluorophenyl)-1,10-dihydropyrrolo[2,3-*a*]carbazole (24). Compound **24** (165 mg, 0.52 mmol, 52%) as a gray−green solid; mp > 250 °C. HRMS (ESI+) calcd for $C_{20}H_{13}F_2N_2$ $(M + H)^+$ 319.1047, found 319.1058. IR (KBr): 3401, 1652, 1616, 1594, 1510 cm^{-1}. ^1H NMR (400 MHz, DMSO-d_6): 6.59 (1H, dd, J_1 = 3.0 Hz, J_2 = 2.0 Hz), 7.21 (1H, tdd, J_1 = 8.5 Hz, J_2 = 3.0 Hz, J_3 = 1.0 Hz), 7.33−7.39 (2H, m), 7.40 (1H, t, J = 2.5 Hz), 7.45 (1H, dt, J_1 = 8.5 Hz, J_2 = 2.0 Hz), 7.67 (1H, td, J_1 = 9.0 Hz, J_2 = 6.5 Hz), 7.69 (1H, d, J = 8.5 Hz), 7.78 (1H, d, J = 8.5 Hz), 8.19 (1H, s), 10.85−10.88 (1H, br s, NH), 11.03−11.06 (1H, br s, NH). ^{13}C NMR (100 MHz, DMSO-d_6): 102.9, 104.3 (dd, J_{CF1} = 27 Hz, J_{CF2} = 26 Hz), 111.3, 111.8 (dd, J_{CF1} = 21 Hz, J_{CF2} = 4 Hz), 112.1, 112.4, 119.4 (d, J_{CF} = 3 Hz), 123.8, 124.3 (d, J_{CF} = 3 Hz), 132.1 (dd, J_{CF1} = 10 Hz, J_{CF2} = 5 Hz) (CH), 116.2, 121.7, 124.4, 124.8 (d, J_{CF} = 1 Hz), 126.3 (dd, J_{CF1} = 14 Hz, J_{CF2} = 4 Hz), 126.5, 126.9, 137.7, 159.1 (dd, J_{CF1} = 247 Hz, J_{CF2} = 12 Hz), 161.1 (dd, J_{CF1} = 246 Hz, J_{CF2} = 12 Hz).

7-(4-Trifluoromethylphenyl)-1,10-dihydropyrrolo[2,3-*a*]carbazole (25). Compound **25** (227 mg, 0.65 mmol, 65%) as a gray solid; mp > 250 °C. HRMS (ESI+) calcd for $C_{21}H_{14}F_3N_2$ $(M + H)^+$ 351.1109, found 351.1125. IR (KBr): 3390, 3362, 1654, 1614 cm^{-1}. ^1H NMR (400 MHz, DMSO-d_6): 6.60 (1H, dd, J_1 = 3.0 Hz, J_2 = 2.0 Hz), 7.39 (1H, d, J = 8.5 Hz), 7.41 (1H, dd, J_1 = 3.0 Hz, J_2 = 2.5 Hz), 7.69 (1H, dd, J_1 = 8.5 Hz, J_2 = 2.0 Hz), 7.73 (1H, dd, J_1 = 8.5 Hz, J_2 = 0.5 Hz), 7.81 (2H, d, J = 8.0 Hz), 7.84 (1H, d, J = 8.5 Hz), 8.01 (2H, d, J = 8.0 Hz), 8.47 (1H, d, J = 1.5 Hz), 10.86−10.92 (1H, br s, NH), 11.06−11.10 (1H, br s, NH). ^{13}C NMR (100 MHz, DMSO-d_6): 102.9, 111.8, 112.2, 112.5, 117.7, 122.6, 123.9, 125.6 (2C, q, J_{CF} = 4 Hz), 127.2 (2C) (CH), 116.3, 121.8, 124.6 (q, J_{CF} = 272 Hz), 124.9, 126.5 (q, J_{CF} = 32 Hz), 126.6, 127.1, 129.3, 138.3, 145.6 (C).

7-(4-Trifluoromethoxyphenyl)-1,10-dihydropyrrolo[2,3-*a*]carbazole (26). Compound **26** (226 mg, 0.62 mmol, 62%) as a gray solid; mp > 250 °C. HRMS (ESI+) calcd for $C_{21}H_{14}F_3N_2O$ $(M + H)^+$ 367.1058, found 367.1044. IR (KBr): 3401, 1652, 1514, 1464 cm^{-1}. ^1H NMR (400 MHz, DMSO-d_6): 6.60 (1H, dd, J_1 = 3.0 Hz, J_2 = 2.0 Hz), 7.37 (1H, d, J = 8.5 Hz), 7.40 (1H, t, J = 2.5 Hz), 7.46 (2H, d, J = 8.0 Hz), 7.62 (1H, dd, J_1 = 8.5 Hz, J_2 = 1.5 Hz), 7.70 (1H, d, J = 8.5 Hz), 7.81 (1H, d, J = 8.5 Hz), 7.87−7.91 (2H, m), 8.38 (1H, d, J = 1.5 Hz), 10.85−10.90 (1H, br s, NH), 11.00−11.05 (1H, br s, NH). ^{13}C NMR (100 MHz, DMSO-d_6): 102.9, 111.7, 112.2, 112.4, 117.5, 121.4 (2C), 122.5, 123.8, 128.3 (CH), 116.3, 120.2 (q, J_{CF} = 256 Hz), 121.8, 124.8, 126.5, 127.0, 129.6, 138.0, 141.0, 147.0 (q, J_{CF} = 2 Hz) (C).

7-(4-Acetylphenyl)-1,10-dihydropyrrolo[2,3-*a*]carbazole (27). Compound **27** (195 mg, 0.60 mmol, 60%) as a brown solid; mp 185 °C (decomposition). HRMS (ESI+) calcd for $C_{22}H_{17}N_2O$ $(M + H)^+$ 325.1341, found 325.1354. IR (KBr): 3700−3100, 1649, 1597 cm^{-1}. ^1H NMR (400 MHz, DMSO-d_6): 2.63 (3H, s, CH_3), 6.59−6.61 (1H, m), 7.38 (1H, d, J = 8.5 Hz), 7.39−7.41 (1H, m), 7.71−7.73 (2H, m), 7.84 (1H, d, J = 8.5 Hz), 7.96 (2H, d, J = 8.5 Hz), 8.06 (2H, d, J = 8.5 Hz), 8.48 (1H, s), 10.86−10.90 (1H, br s, NH), 11.05−11.08 (1H, br s, NH). ^{13}C NMR (100 MHz, DMSO-d_6): 26.7 (CH_3), 102.9, 111.8, 112.2, 112.5, 117.7, 122.6, 123.9, 126.5 (2C), 128.9 (2C) (CH), 116.3, 121.7, 124.9, 126.6, 127.0, 129.6, 134.5, 138.3, 146.1 (C), 197.4 (C=O).

7-Bromo-1,10-dihydropyrrolo[2,3-*a*]carbazole-3-carbaldehyde (28). A mixture of oxalyl chloride (32.5 μL, 0.38 mmol) and DMF (31 μL, 0.40 mmol) in dichloromethane (10 mL) was stirred at 0 °C for 20 min. A solution of **19** (100 mg, 0.35 mmol) in dichloromethane (10 mL) was added dropwise. The mixture was stirred at 0 °C for 20 min before reaching room temperature. The solvent was evaporated and a 5% aq NaOH solution (20 mL) was added. The mixture was stirred for 12 h and then extracted with EtOAc. The organic phase was washed with water, brine, dried over $MgSO_4$, and evaporated. The residue was purified by flash chromatography (cyclohexane/EtoAc 7:3 then 5:5) to give **28** (72 mg, 0.230 mmol, 66%) as a gray solid; mp > 250 °C. HRMS (ESI+) calcd for $C_{15}H_{10}{}^{79}BrN_2O$ $(M + H)^+$ 312.9976, found 312.9979. IR (KBr): 3400−3100, 1630 cm^{-1}. ^1H NMR (400 MHz, DMSO-d_6): 7.48 (1H, dd, J_1 = 8.5 Hz, J_2 = 2.0 Hz), 7.65 (1H, d, J = 8.5 Hz), 7.94 (1H, d, J = 8.5 Hz), 8.00 (1H, d, J = 8.5 Hz), 8.31 (1H, d, J = 3.0 Hz), 8.34 (1H, d, J = 2.0 Hz), 10.04 (1H, s), 11.18−11.23 (1H, br s, NH), 11.89−11.96 (1H, br s, NH). ^{13}C NMR (100 MHz, DMSO-d_6): 112.6, 113.5, 115.3, 122.0, 126.6, 137.0 (CH), 111.2, 117.4, 119.5, 122.5, 123.1, 125.5, 126.6, 137.2 (C), 185.4 (C=O). HPLC purity, system I: >96%, λ = 264 nm, t_R = 23.9 min.

7-(3-Methoxyphenyl)-1,10-dihydropyrrolo[2,3-*a*]carbazole-3-carbaldehyde (29). $POCl_3$ (90 μL, 0.97 mmol) was slowly added to anhyd DMF (2 mL) at 0 °C. The mixture was stirred at 0−10 °C for 45 min until a yellow solution was obtained. A solution of **20** (100 mg, 0.320 mmol) in DMF (1 mL) was then added. The mixture was heated at 120 °C for 24 h. After cooling, a 5% aq NaOH solution (20 mL) was added and the mixture was stirred at room temperature overnight. After extraction with EtOAc, the organic phase was dried over $MgSO_4$, evaporated, and the residue was purified by flash chromatography (pentane/EtOAc, from 7:3 to 1:9) to give **29** (49 mg, 0.144 mmol, 45%) as a light-brown solid; mp 215 °C (decomposition). HRMS (ESI+) calcd for $C_{22}H_{17}N_2O_2$ $(M + H)^+$ 341.1290, found 341.1305. IR (KBr): 3325, 1619 cm^{-1}. ^1H NMR (400 MHz, DMSO-d_6): 3.87 (3H, s, CH_3), 6.91 (1H, d, J = 7.5 Hz), 7.31−7.42 (3H, m), 7.69 (1H, dd, J_1 = 8.5 Hz, J_2 = 1.5 Hz), 7.74 (1H, d, J = 8.5 Hz), 7.95 (1H, d, J = 8.5 Hz), 8.08 (1H, d, J = 8.5 Hz), 8.31 (1H, d, J = 3.0 Hz), 8.45 (1H, s), 10.04 (1H, s), 11.09−11.13 (1H, br s, NH), 11.88−11.92 (1H, br s, NH). ^{13}C NMR (100 MHz, DMSO-d_6): 55.1 (CH_3), 111.8, 112.0, 112.2 (2C), 115.3, 117.8, 119.1, 123.5, 129.8, 136.9 (CH), 118.6, 119.6, 122.8 (2C), 124.1, 126.5, 131.4, 138.2, 142.9, 159.7 (C), 185.3 (C=O). HPLC purity, system I: >96%, λ = 267 nm, t_R = 24.0 min.

General Procedure for the Preparation of Compounds (30−35). $POCl_3$ (3 equiv) was slowly added to anhyd DMF (2 mL) at 0 °C. The solution was stirred at 0−10 °C for 45 min until a yellow solution was obtained, and then was added to a solution of compound **21**−**27** (100 mg) in DMF (1 mL) at 0 °C prepared in a 10 mL CEM reaction vessel. The tube was sealed and was heated at 100 °C under microwave irradiation for 20 min (150 W). After cooling, the mixture was poured into a saturated aq $NaHCO_3$ solution (20 mL). After 30 min of stirring, the solid was filtered off and a 5% aq NaOH solution (20 mL) was added. The mixture was stirred at room temperature overnight. The solid was filtered off and then purified by flash chromatography (pentane/EtOAc, from 7:3 to 1:9).

7-Phenyl-1,10-dihydropyrrolo[2,3-*a*]carbazole-3-carbaldehyde (30). Compound **30** (57 mg, 0.184 mmol, 52%) as a dark-brown solid; mp 205 °C (decomposition). HRMS (ESI+) calcd for $C_{21}H_{15}N_2O$ $(M + H)^+$ 311.1184, found 311.1201. IR (KBr): 3260, 1622 cm^{-1}. ^1H NMR (400 MHz, DMSO-d_6): 7.31−7.36 (1H, m), 7.46−7.51 (2H, m), 7.68 (1H, dd, J_1 = 8.5 Hz, J_2 = 2.0 Hz), 7.75 (1H, dd, J_1 = 8.5 Hz, J_2 = 0.5 Hz), 7.77−7.81 (2H, m), 7.95 (1H, d, J = 8.5 Hz), 8.06 (1H, d, J = 8.5 Hz), 8.31 (1H, d, J = 3.0 Hz), 8.43 (1H, d, J = 2.0 Hz), 10.04 (1H, s), 11.08−11.14 (1H,

br s, NH), 11.86−11.93 (1H, br s, NH). ^{13}C NMR (100 MHz, DMSO-d_6): 111.9, 112.3, 115.3, 117.7, 123.4, 126.4, 126.7 (2C), 128.8 (2C), 136.9 (CH), 118.6, 119.6, 122.8 (2C), 124.2, 126.5, 131.5, 138.1, 141.4 (C), 185.4 (C=O). HPLC purity, system I: >96%, λ = 268 nm, t_R = 24.8 min.

7-(4-Biphenyl)-1,10-dihydropyrrolo[2,3-*a*]carbazole-3-carbaldehyde (31). Compound **31** (32 mg, 0.083 mmol, 30%) as a dark-brown solid; mp > 250 °C. HRMS (ESI+) calcd for $C_{27}H_{19}N_2O$ $(M + H)^+$ 387.1497, found 387.1492. IR (KBr): 3436, 1622 cm^{-1}. ^{1}H NMR (400 MHz, DMSO-d_6): 7.36−7.41 (1H, m), 7.47−7.52 (2H, m), 7.73−7.81 (6H, m), 7.88−7.92 (2H, m), 7.96 (1H, d, J = 8.5 Hz), 8.09 (1H, d, J = 8.5 Hz), 8.31 (1H, d, J = 3.0 Hz), 8.51 (1H, s), 10.05 (1H, s), 11.12−11.16 (1H, br s, NH), 11.90 (1H, br d, J = 2.5 Hz, NH). ^{13}C NMR (100 MHz, DMSO-d_6): 112.0, 112.3, 115.3, 117.5, 123.3, 126.5 (2C), 127.1 (4C), 127.3, 129.0 (2C), 136.9 (CH), 118.6, 119.6, 122.8 (2C), 124.2, 126.5, 130.9, 138.0, 138.2, 139.8, 140.4 (C), 185.3 (C=O). HPLC purity, system I: >97%, λ = 310 nm, t_R = 27.8 min.

7-(4-Fluorophenyl)-1,10-dihydropyrrolo[2,3-*a*]carbazole-3-carbaldehyde (32). Compound **32** (55 mg, 0.168 mmol, 50%) as a light-brown solid; mp > 250 °C. HRMS (ESI+) calcd for $C_{21}H_{14}N_2OF$ $(M + H)^+$ 329.1090, found 329.1101. IR (KBr): 3436, 3297, 1619 cm^{-1}. ^{1}H NMR (400 MHz, DMSO-d_6): 7.27−7.34 (2H, m), 7.65 (1H, dd, J_1 = 8.5 Hz, J_2 = 2.0 Hz), 7.74 (1H, d, J = 8.5 Hz), 7.78−7.84 (2H, m), 7.95 (1H, d, J = 8.5 Hz), 8.06 (1H, d, J = 8.5 Hz), 8.31 (1H, s), 8.41 (1H, d, J = 1.5 Hz), 10.04 (1H, s), 11.10−11.15 (1H, br s, NH), 11.88−11.95 (1H, br s, NH). ^{13}C NMR (100 MHz, DMSO-d_6): 112.0, 112.3, 115.3, 115.6 (2C, d, J_{CF} = 21 Hz), 117.7, 123.4, 128.5 (2C, d, J_{CF} = 8 Hz), 136.9 (CH), 118.6, 119.6, 122.8 (2C), 124.2, 126.6, 130.6, 137.9 (d, J_{CF} = 3 Hz), 138.1, 161.3 (d, J_{CF} = 243 Hz), 185.4 (C=O). HPLC purity, system I: >96%, λ = 267 nm, t_R = 25.0 min.

7-(2,4-Difluorophenyl)-1,10-dihydropyrrolo[2,3-*a*]carbazole-3-carbaldehyde (33). Compound **33** (48 mg, 0.139 mmol, 44%) as a beige solid; mp 220 °C (decomposition). HRMS (ESI+) calcd for $C_{21}H_{13}F_2N_2O$ $(M + H)^+$ 347.0996, found 347.0996. IR (KBr): 3264, 1645, 1616 cm^{-1}. ^{1}H NMR (400 MHz, DMSO-d_6): 7.22 (1H, td, J_1 = 8.5 Hz, J_2 = 2.5 Hz), 7.37 (1H, ddd, J_1 = 11.5 Hz, J_2 = 9.5 Hz, J_3 = 2.5 Hz), 7.52 (1H, dt, J_1 = 8.5 Hz, J_2 = 2.0 Hz), 7.69 (1H, td, J_1 = 9.0 Hz, J_2 = 7.0 Hz), 7.76 (1H, d, J = 8.5 Hz), 7.95 (1H, d, J = 8.5 Hz), 8.02 (1H, d, J = 8.5 Hz), 8.27 (1H, s), 8.31 (1H, s), 10.04 (1H, s), 11.19−11.26 (1H, br s, NH), 11.90−12.01 (1H, br s, NH). ^{13}C NMR (100 MHz, DMSO-d_6): 104.3 (dd, J_{CF1} = 27 Hz, J_{CF2} = 26 Hz), 111.6, 111.8 (dd, J_{CF1} = 21 Hz, J_{CF2} = 4 Hz), 112.4, 115.2, 119.9 (d, J_{CF} = 2 Hz), 125.2, 132.1 (dd, J_{CF1} = 9 Hz, J_{CF2} = 5 Hz), 136.9 (CH), 118.3, 119.6, 122.8 (2C), 123.8, 125.2, 126.1 (dd, J_{CF1} = 14 Hz, J_{CF2} = 4 Hz), 126.5, 138.1, 159.1 (dd, J_{CF1} = 247 Hz, J_{CF2} = 12 Hz), 161.1 (dd, J_{CF1} = 246 Hz, J_{CF2} = 12 Hz (C), 185.3 (C=O). HPLC purity, system I: >97%, λ = 264 nm, t_R = 25.2 min.

7-(4-Trifluoromethylphenyl)-1,10-dihydropyrrolo[2,3-*a*]carbazole-3-carbaldehyde (34). Compound **34** (70 mg, 0.185 mmol, 65%) as a light-brown solid; mp > 250 °C. HRMS (ESI+) calcd for $C_{22}H_{14}F_3N_2O$ $(M + H)^+$ 379.1058, found 379.1059. IR (KBr): 3460, 3294, 1617 cm^{-1}. ^{1}H NMR (400 MHz, DMSO-d_6): 7.76 (1H, dd, J_1 = 8.5 Hz, J_2 = 1.5 Hz), 7.80 (1H, dd, J_1 = 8.5 Hz, J_2 = 1.0 Hz), 7.83 (2H, d, J = 8.0 Hz), 7.97 (1H, d, J = 8.5 Hz), 8.03 (2H, d, J = 8.0 Hz), 8.09 (1H, d, J = 8.5 Hz), 8.32 (1H, s), 8.56 (1H, s), 10.04 (1H, s), 11.18−11.25 (1H, br s, NH), 11.88−11.97 (1H, br s, NH). ^{13}C NMR (100 MHz, DMSO-d_6): 112.2, 112.5, 115.3, 118.2, 123.5, 125.7 (2C, q, J_{CF} = 4 Hz), 127.3 (2C), 137.0 (CH), 118.5, 119.6, 122.8, 122.9, 124.3, 124.6 (q, J_{CF} = 272 Hz), 126.6, 126.7 (q, J_{CF} = 32 Hz), 129.7, 138.7, 145.4 (C), 185.4 (C=O). HPLC purity, system I: >95%, λ = 287 nm, t_R = 26.5 min.

7-(4-Trifluoromethoxyphenyl)-1,10-dihydropyrrolo[2,3-*a*]carbazole-3-carbaldehyde (35). Compound **35** (72 mg, 0.183 mmol, 67%) as a beige solid; mp > 250 °C. HRMS (ESI+) calcd for $C_{22}H_{14}F_3N_2O_2$ $(M + H)^+$ 395.1007, found 395.1017. IR (KBr): 3276, 1620 cm^{-1}. ^{1}H NMR (500 MHz, DMSO-d_6): 7.46 (2H, d, J = 8.5 Hz), 7.69 (1H, dd, J_1 = 8.5 Hz, J_2 = 2.0 Hz), 7.75 (1H, d, J = 8.5 Hz), 7.88−7.92 (2H, m), 7.95 (1H, d, J = 8.5 Hz), 8.06 (1H, d, J = 8.5 Hz), 8.31 (1H, d, J = 3.0 Hz), 8.46 (1H, d, J = 2.0 Hz), 10.03 (1H, s), 11.15−11.18 (1H, br s, NH), 11.93 (1H, br d, J = 2.5 Hz, NH). ^{13}C NMR (125 MHz, DMSO-d_6): 112.1, 112.5, 115.4, 118.0, 121.5 (2C), 123.6, 128.5 (2C), 137.0 (CH), 118.6, 119.7, 120.3 (q, J_{CF} = 256 Hz), 122.9, 123.0, 124.3, 126.7, 130.1, 138.4, 140.8, 147.2 (q, J_{CF} = 2 Hz) (C), 185.5 (C=O). HPLC purity, system I: >95%, λ = 270 nm, t_R = 24.9 min.

In Vitro Kinase Inhibition Assays. The procedures for the in vitro protein kinase assays and for the expression and activation of the protein kinases have been detailed previously.[40]

Source and Purification of Kinases. All protein kinases were of human origin and encoded full-length proteins except for RSK1, ROCK2, CK1δ, and AMPK (rat), ERK2 and lck (mouse), and MKK1 (rabbit). Apart from the AMPK (AMP-activated protein kinase) complex, which was purified from rat liver, all other proteins were either expressed as GST (glutathione transferase) fusion proteins in *Escherichia coli* or as hexahistidine (His_6)-tagged proteins in Sf21 (*Spodoptera frugiperda* 21) insect cells. GST fusion proteins were purified by affinity chromatography on glutathione−Sepharose, and His_6-tagged proteins on nickel/nitrilotriacetate−agarose.

Protein Kinase Assays. All assays (25.5 μL volume) were carried out robotically at room temperature (21 °C) and were linear with respect to time and enzyme concentration under the conditions used. Assays were performed for 30 min using Multidrop Micro reagent dispensers (Thermo Electron Corporation, Waltham, MA) in a 96-well format. The concentration of magnesium acetate in the assays was 10 mM and [γ-^{33}P]ATP (800 cpm/pmol) was used at 5, 20, or 50 μM as indicated in order to be at or below the K_m for ATP for each enzyme. Protein kinases assayed at 5 μM ATP were: MKK1, ERK1, p38γ MAPK, p38δ MAPK, ERK8, PKBα, PKCζ, PRK2, GSK3β, CK2, MARK3, IKKβ, PIM2, EF2K, PLK1, Aurora C, HIPK2, and PAK4. Protein kinases assayed at 20 μM ATP were: JNK1, JNK2, p38β MAPK, PDK1, SGK1, S6K1, PKA, ROCK2, PKCα, MSK1, MAPKAP-K2, MAPKAP-K3, PRAK, CaMKKα, CaMKKβ, CHK1, CHK2, CDK2, Aurora B, CK1, PIM1, PIM3, NEK7, MST2, HIPK3, PAK5, PAK6, CSK. Protein kinases assayed at 50 μM ATP were: ERK2, JNK3, p38α MAPK, RSK1, RSK2, PKBβ, PKD1, MNK1, MNK2, AMPK, CaMK1, smMLCK, PHK, BRSK2, MELK, NEK2a, NEK6, SRPK1, Src, Lck.

The assays were initiated with MgATP, stopped by the addition of 5 μL of 0.5 M orthophosphoric acid, and spotted on to P81 filter plates using a unifilter harvester (PerkinElmer, Boston, MA).

Kinase substrates were: PKA, (single-letter code for amino acids) LRRASLG (300 μM); PKCα, protein histone H1 (0.1 mg/mL); PHK, KRKQISVRGL (300 μM); CK1, RRKDLHDDEEDEAMSITA (0.5 mM); NEK2a, RFRRSRRMI (300 μM); NEK6 and NEK7, FLAKSFGSPNRAYKK (300 μM), ROCK2 and PRK2, KEAKEKRQEQIAKRRRLSSLRASTSKSGGSQK (peptide corresponding to the C-terminal region of ribosomal protein S6; 30 μM); Aurora B and Aurora C, LRRLSLGLRRLSLGLRRLSLGLRRLSLG (300 μM); ERK1, ERK2, ERK8, HIPK2, HIPK3 and MST2, p38α MAPK, p38β MAPK, p38γ MAPK, and p38δ MAPK, MBP (myelin basic protein; 0.33 mg/mL); IKKβ, LDDRHDSGLDSMKDEEY (300 μM); JNK1, JNK2, and JNK3, ATF2-[19−96] (activating transcription factor 2[19−96]; 3 μM); MARK3, KKKVSRSGLYRSPSMPENLNRPR (300 μM); RSK1, RSK2, MAPKAP-K3, and PKD1, KKLNRTLSVA (30 μM); MNK1 and MNK2, eIF4E (eukaryotic translation initiation factor 4E) protein (0.5 mg/mL); EF2K, RKKFGESKTKTKEFL (300 μM); Pim-1, Pim-2, and Pim-3, RSRHSSYPAGT (300 μM); SGK1 and PKBβ, GRPRTSSFAEGKK (30 μM); PLK1, ISDELMDATFADQEAKKK

(300 μM); Src, KVEKIGEGTYGVVYK (300 μM), CaMK1, YLRRRLSDSNF (300 μM); smMLCK, KKRPQRATSNVFA (300 μM); SRPK1, RSRSRSRSRSRSRSR (300 μM); PAK4, 5, and 6, RRRLSFAEPG (300 μM); CaMKKα and CaMKKβ, AKPKGNKDYHLQTCCGSLAYRRR (300 μM); MELK and BRSK2, KKLNRTLSFAEPG (300 μM); PKCζ, ERMRPRKRQGSVRRV (300 μM); CHK1 and CHK2, KKKVSRSGLYRSPSMPENLNRPR (200 μM); MAPKAP-K2, KKLNRTLSVA (30 μM); PRAK, KKLRRTLSVA (30 μM); PDK1, against KTFCGTPEYLAPEVRREPRILSEEEQEMFRDFDYIADWC (PDKtide; 0.1 mM); PKBα against GRPRTSSFAEG (30 μM); S6K1, KKRNRTLTV (100 μM); MSK1, GRPRTSSFAEG (30 μM); AMPK, HMRSAMSGLHLVKRR (0.2 mM); CK2, RRRDDDSDDD (165 μM); Lck, KVEKIGEGTYGVVYK (250 μM); CDK2, protein histone H1 (1 mg/mL); GSK3β, YRRAAVPPSPSLSRHSSPHQS(PO_4)-EDEEE (20 μM); CSK, KVEKIGEGTYGVVYK (0.25 mM); MKK1 was assayed via its ability to activate ERK2 (0.07 mg/mL).

Unless stated otherwise, enzymes were diluted in a buffer consisting of 50 mM Tris/HCl, pH 7.5, 0.1 mM EGTA, 1 mg/mL BSA, and 0.1% 2-mercaptoethanol and assayed in a buffer comprising 50 mM Tris/HCl, pH 7.5, 0.1 mM EGTA, and 0.1% 2-mercaptoethanol. For CaMK1 and CaMKK isoforms, the assay mixtures also contained 0.5 mM $CaCl_2$ and 0.3 μM calmodulin. PKCα was diluted into 20 mM Hepes (pH 7.4)/0.03 Triton X-100 and assayed in the same buffer containing 0.1 mg/mL phosphatidylserine, 10 μg/mL diacylglycerol, and 0.1 mM $CaCl_2$. PHK (5−20 m-units) was diluted in 50 mM sodium β-glycerophosphate (pH 7.0)/0.1% 2-mercaptoethanol and assayed in a buffer comprising 50 mM Tris/HCl, 50 mM sodium β-glycerophosphate, pH 8.2, and 0.04 mM $CaCl_2$. EF2K (5−20 m-units) was diluted into 50 mM Hepes (pH 6.6)/0.1% 2-mercaptoethanol/1.0 mg/mL BSA and assayed in the same buffer containing 0.2 mM $CaCl_2$ and 0.3 μM calmodulin. smMLCK (5−20 m-units) was diluted in 50 mM Hepes (pH 7.5)/0.1 mM EGTA/1.0 mg/mL BSA/0.1% 2-mercaptoethanol and assayed in the same buffer containing 5 mM $CaCl_2$ and 10 μM calmodulin. PKA (5−20 m-units) was diluted in 20 mM Mops (pH 7.5)/1 mM EGTA/0.01% Brij-35/1.0 mg/mL BSA/0.1% 2-mercaptoethanol and assayed in 8 mM Mops (pH 7.5)/0.2 mM EDTA. MKK1 was assayed via its ability to activate ERK2 in incubations containing 25 mM Tris/HCl, pH 7.5, 0.1 mM EGTA, 0.1% 2-mercaptoethanol, 0.01% Brij-35 and MgATP.[46] After incubation for 15 min at 30 °C, activated ERK2 was assayed as described above.

The inhibition profile of the tested compounds was expressed as the percentage of the residual kinase activity for an inhibitor concentration of 1 or 10 μM. The IC_{50} values of inhibitors were determined after carrying out assays at 10 different concentrations of each compound. The results are shown as standard errors for duplicate determinations.

Crystallography. Protein Purification. Pim-1 was prepared as previously described.[42] The protein was >95% pure as judged by SDS-PAGE. The purified protein was homogeneous and had an experimental mass of 35545 Da as expected from its primary structure. Masses were determined by LC-MS, using an Agilent LC/MSD TOF system with reversed-phase HPLC coupled to electrospray ionization and an orthogonal time-of-flight mass analyzer. Proteins were desalted prior to mass spectrometry by rapid elution off a C3 column with a gradient of 5−95% acetonitrile in water with 0.1% formic acid.

Crystallization, Data Collection, and Structure Solution. Crystallization was carried out using the sitting drop vapor diffusion method at 4 °C. A 6 mL solution with 1 mg of PIM1 buffered in 50 mM Hepes pH 7.5, 250 mM NaCl, 10 mM DTT was prepared containing 2 μL of inhibitor (from a 50 mM stock in DMSO) and 20 μL of a 5 mM solution of consensus peptide (ARKRRRHPSGPPTA-amide). This sample was then concentrated to 100 μL to yield a 10 mg/mL crystal sample. Crystals of the complex were grown by mixing 150 nL of the protein (5 mg/mL) with an equal volume of reservoir solution containing 0.2 M NaF, 100 mM bistrispropane pH 8.5, 20% PEG3350, and 10% ethylene glycol. Crystals grew to diffracting quality within a few days. Crystals were cryoprotected using the well solution supplemented with additional ethylene glycol and were flash frozen in liquid nitrogen. Data were collected at a Rigaku FRE Superbright equipped with an RAXIS IV detector at 1.5 Å. Indexing and integration was carried out using MOSFLM,[47] and scaling was performed with SCALA.[48] Initial phases were calculated by molecular replacement with PHASER[49] using 2C3I as a starting model. The model was completed manually in COOT[50] and was refined with REFMAC5.[51] Thermal motions were analyzed using TLSMD[52] and hydrogen atoms were included in late refinement cycles. Data collection and refinement statistics can be found in Table 4. The model and structure factors have been deposited with PDB accession code: 3JPV.

In Vitro Antiproliferative Assays. Cell Cultures. Stock cell cultures were maintained as monolayers in 75 cm^2 culture flasks in Glutamax Eagle's minimum essential medium (MEM) with Earle's salts supplemented with 10% fetal calf serum, 5 mL 100 mM sodium pyruvate, 5 mL of 100X nonessential amino acids and 2 mg gentamicin base. Cells were grown at 37 °C in a humidified incubator under an atmosphere containing 5% CO_2.

Survival Assays. Cells were plated at a density of 5×10^3 cells in 150 μL of culture medium in each well of 96-well microplates and were allowed to adhere for 16 h before treatment with tested drug. A stock solution 20 mM of each tested drug was prepared in DMSO and kept at −20 °C until use. Then 50 μL of each tested solution were added to the cultures. A 48 h continuous drug exposure protocol was used. The antiproliferative effect of the tested drug was assessed by the resazurin reduction test.

Resazurin Reduction Test. Plates were rinsed with 200 μL of PBS at 37 °C and emptied by overturning on absorbent toweling. Then 150 μL of a 25 μg/mL solution of resazurin in MEM without phenol red was added to each well. Plates were incubated for 1 h at 37 °C in a humidified atmosphere containing 5% CO_2. Fluorescence was then measured on an automated 96-well plate reader (Fluoroscan Ascent FL, Labsystem) using an excitation wavelength of 530 nm and an emission wavelength of 590 nm. Under the conditions used, fluorescence was proportional to the number of living cells in the well. The IC_{50}, defined as the drug concentration required to inhibit cell proliferation by 50%, was calculated from the curve of concentration-dependent survival percentage, defined as fluorescence in experimental wells compared with fluorescence in control wells, after subtraction of the blank values. The results are shown as standard errors for duplicate determinations.

Acknowledgment. We are grateful to the European Union ProKinase Research Consortium and CNRS Valorisation for financial support. We thank the Kinase Profiling Service of the Division of Signal Transduction Therapy, MRC Protein Phosphorylation Unit, University of Dundee (managed by Jenny Bain), for performing the protein kinase assays. We also thank Bertrand Légeret for mass spectra analysis and Aurélie Job for technical assistance for HPLC analysis. The Structural Genomics Consortium is a registered charity (no. 1097737) that receives funds from the Canadian Institutes for Health Research, the Canadian Foundation for Innovation, Genome Canada, through the Ontario Genomics Institute, GlaxoSmithKline, Karolinska Institutet, the Knut and Alice Wallenberg Foundation, the Ontario Innovation Trust, the Ontario Ministry for Research and Innovation, Merck & Co. Inc., the Novartis Research Foundation, the Swedish Agency for Innovation Systems, the Swedish Foundation for Strategic Research, and the Wellcome Trust.

References

(1) Saris, C. J.; Domen, J.; Berns, A. The pim-1 oncogene encodes two related protein-serine/threonine kinases by alternative initiation at AUG and CUG. *EMBO J.* **1991**, *10*, 655–664.

(2) Hoover, D.; Friedmann, M.; Reeves, R.; Magnuson, N. S. Recombinant human pim-1 protein exhibits serine/threonine kinase activity. *J. Biol. Chem.* **1991**, *266*, 14018–14023.

(3) van der Lugt, N. M.; Domen, J.; Verhoeven, E.; Linders, K. van der Gulden, H.; Allen, J.; Berns, A. Proviral tagging in E mu-myc transgenic mice lacking the Pim-1 proto-oncogene leads to compensatory activation of Pim-2. *EMBO J.* **1995**, *14*, 2536–2544.

(4) Cuypers, H. T.; Selten, G.; Quint, W.; Zijlstra, M.; Maandag, E. R.; Boelens, W.; van Wezenbeek, P.; Melief, C.; Berns, A. Murine leukemia virus-induced T-cell lymphomagenesis: integration of proviruses in a distinct chromosomal region. *Cell* **1984**, *37*, 141–150.

(5) Mikkers, H.; Nawijn, M.; Allen, J.; Brouwers, C.; Verhoeven, E.; Jonkers, J.; Berns, A. Mice Deficient for all PIM kinases display reduced body size and impaired responses to hematopoietic growth factors. *Mol. Cell. Biol.* **2004**, *24*, 6104–6115.

(6) Shah, N.; Pang, B.; Yeoh, K.-G.; Thorn, S.; Chen, C. S.; Lilly, M. B.; Salto-Tellez, M. Potential roles for the PIM1 kinase in human cancer − a molecular and therapeutic appraisal. *Eur. J. Cancer* **2008**, 2144–2151.

(7) Morishita, D.; Katayama, R.; Sekimizu, K.; Tsuruo, T.; Fujita, N. Pim kinases promote cell cycle progression by phosphorylating and down-regulating $p27^{Kip1}$ at the transcriptional and posttranscriptional levels. *Cancer Res.* **2008**, *68*, 5076–5085.

(8) Peng, C.; Knebel, A.; Morrice, N. A.; Li, X.; Barringer, K.; Li, J.; Jakes, S.; Werneburg, B.; Wang, L. Pim Kinase Substrate Identification and Specificity. *J. Biochem.* **2007**, *141*, 353–362.

(9) Bachmann, M.; Kosan, C.; Xing, P. X.; Montenarh, M.; Hoffmann, I.; Moroy, T. The oncogenic serine/threonine kinase Pim-1 directly phosphorylates and activates the G2/M specific phosphatase Cdc25C. *Int. J. Biochem. Cell Biol.* **2006**, *38*, 430–443.

(10) Bachmann, M.; Moroy, T. The serine/threonine kinase Pim-1. *Int. J. Biochem. Cell Biol.* **2005**, *37*, 726–730.

(11) Fox, C. J.; Hammerman, P. S.; Cinalli, R. M.; Master, S. R.; Chodosh, L. A.; Thompson, C. B. The serine/threonine kinase Pim-2 is a transcriptionally regulated apoptotic inhibitor. *Genes Dev.* **2003**, *17*, 1841–1854.

(12) Aho, T. L.; Sandholm, J.; Peltola, K. J.; Ito, Y.; Koskinen, P. J. Pim-1 kinase phosphorylates RUNX family transcription factors and enhances their activity. *BMC Cell Biol.* **2006**, *7*, 21.

(13) Peltola, K. J.; Paukku, K.; Aho, T. L.; Ruuska, M.; Silvennoinen, O.; Koskinen, P. J. Pim-1 kinase inhibits STAT5-dependent transcription via its interactions with SOCS1 and SOCS3. *Blood* **2004**, *103*, 3744–3750.

(14) Aho, T. L.; Sandholm, J.; Peltola, K. J.; Mankonen, H. P.; Lilly, M.; Koskinen, P. J. Pim-1 kinase promotes inactivation of the pro-apoptotic Bad protein by phosphorylating it on the Ser112 gatekeeper site. *FEBS Lett.* **2004**, *571*, 43–49.

(15) Zheng, H.-C.; Tsuneyama, K.; Takahashi, H.; Miwa, S.; Sugiyama, T.; Popivanova, B. K.; Fujii, C.; Nomoto, K.; Mukaida, N.; Takano, Y. Aberrant Pim-3 expression is involved in gastric adenoma−adenocarcinoma sequence and cancer progression. *J. Cancer Res. Clin. Oncol.* **2008**, *134*, 481–488.

(16) Li, Y.-Y.; Wu, Y.; Tsuneyama, K.; Baba, T.; Mukaida, N. Essential contribution of Ets-1 to constitutive Pim-3 expression in human pancreatic cancer cells. *Cancer Sci.* **2009**, *100*, 396–404.

(17) Popivanova, B. K.; Li, Y.-Y.; Zheng, H.; Omura, K.; Fujii, C.; Tsuneyama, K.; Mukaida, N. Proto-oncogene, Pim-3 with serine/threonine kinase activity, is aberrantly expressed in human colon cancer cells and can prevent Bad-mediated apoptosis. *Cancer Sci.* **2007**, *98*, 321–329.

(18) Li, Y.-Y.; Popivanova, B. K.; Nagai, Y.; Ishikura, H.; Fujii, C.; Mukaida, N. Pim-3, a proto-oncogene with serine/threonine kinase activity, is aberrantly expressed in human pancreatic cancer and phosphorylates Bad to block Bad-mediated apoptosis in human pancreatic cancer cell lines. *Cancer Res.* **2006**, *66*, 6741–6747.

(19) Adam, M.; Pogacic, V.; Bendit, M.; Chappuis, R.; Nawijn, M. C.; Duyster, J.; Fox, C. J.; Thompson, C. B.; Cools, J.; Schwaller, J. Targeting PIM kinases impairs survival of hematopoietic cells transformed by kinase inhibitor-sensitive and kinase inhibitor-resistant forms of Fms-like tyrosine kinase 3 and BCR/ABL. *Cancer Res.* **2006**, *66*, 3828–3835.

(20) Hammerman, P. S.; Fox, C. J.; Birnbaum, M. J.; Thompson, C. B. Pim and Akt oncogenes are independent regulators of hematopoietic cell growth and survival. *Blood* **2005**, *105*, 4477–4483.

(21) Giles, F. A Pim kinase inhibitor, please. *Blood* **2005**, *105*, 4158–4159.

(22) Holder, S.; Zemskova, M.; Zhang, C.; Tabrizizad, M.; Bremer, R.; Neidigh, J. W.; Lilly, M. B. Characterization of a potent and selective small-molecule inhibitor of the PIM1 kinase. *Mol. Cancer Ther.* **2007**, *6*, 163–172.

(23) Pogacic, V.; Bullock, A. N.; Fedorov, O.; Filippakopoulos, P.; Gasser, C.; Biondi, A.; Meyer-Monard, S.; Knapp, S.; Schwaller, J. Structural analysis identifies imidazo[1,2-*b*]pyridazines as PIM kinase inhibitors with in vitro antileukemic activity. *Cancer Res.* **2007**, *67*, 6916–6924.

(24) Grey, R.; Pierce, A. C.; Bemis, G. W.; Jacobs, M. D.; Moody, C. S.; Jajoo, R.; Mohal, N.; Green, J. Structure-based design of 3-aryl-6-amino-triazolo[4,3-*b*]pyridazine inhibitors of Pim-1 kinase. *Bioorg. Med. Chem. Lett.* **2009**, *19*, 3019–3022.

(25) Anand, R.; Maksimoska, J.; Pagano, N.; Wong, E. Y.; Gimotty, P. A.; Diamond, S. L.; Meggers, E.; Marmorstein, R. Toward the development of a potent and selective organoruthenium mammalian sterile 20 kinase inhibitor. *J. Med. Chem.* **2009**, *52*, 1602–1611.

(26) Meggers, E.; Atilla-Gokcumen, G. E.; Bregman, H.; Maksimoska, J.; Mulcahy, S. P.; Pagano, N.; Williams, D. S. Exploring chemical space with organometallics: ruthenium complexes as protein kinase inhibitors. *Synlett* **2007**, 1177–1189.

(27) Tong, Y.; Stewart, K. D.; Thomas, S.; Przytulinska, M.; Johnson, E. F.; Klinghofer, V.; Leverson, J.; McCall, O.; Soni, N. B.; Luo, Y.; Lin, N.-H.; Sowin, T. J.; Giranda, V. L.; Penning, T. D. Isoxazolo[3,4-*b*]quinoline-3,4(1*H*,9*H*)-diones as unique, potent and selective inhibitors for Pim-1 and Pim-2 kinases: chemistry, biological activities, and molecular modelling. *Bioorg. Med. Chem. Lett.* **2008**, *18*, 5206–5208.

(28) Xia, Z.; Knaak, C.; Ma, J.; Beharry, Z. M.; McInnes, C.; Wang, W.; Kraft, A. S.; Smith, C. D. Synthesis and evaluation of novel inhibitors of Pim-1 and Pim-2 protein kinases. *J. Med. Chem.* **2009**, *52*, 74–86.

(29) Qian, K.; Wang, L.; Cywin, C. L.; Farmer, B. T.; Hickey, E.; Homon, C.; Jakes, S.; Kashem, M. A.; Lee, G.; Leonard, S.; Li, J.; Magboo, R.; Mao, W.; Pack, E.; Peng, C.; Prokopowicz, A.; Welzel, M.; Wolak, J.; Morwick, T. Hit to lead account of the discovery of a new class of inhibitors of Pim kinases and crystallographic studies revealing an unusual kinase binding mode. *J. Med. Chem.* **2009**, *52*, 1814–1827.

(30) Fousteris, M. A.; Papakyriakou, A.; Koutsourea, A.; Manioudaki, M.; Lampropoulou, E.; Papadimitriou, E.; Spyroulias, G. A.; Nikolaropoulos, S. S. Pyrrolo[2,3-*a*]carbazoles as potential cyclin dependent kinase 1 (CDK1) inhibitors. Synthesis, biological evaluation, and binding mode through docking simulations. *J. Med. Chem.* **2008**, *51*, 1048–1052.

(31) Sikharulidze, M. I.; Khoshtariya, T. E.; Kurkovskaya, L. N.; Tret'yakova, L. G.; Efimova, T. K.; Suvorov, N. N. Pyrrolocarbazoles. 3. Synthesis and spectral properties of 1*H*-pyrrolo[2,3-*a*]-carbazole. *Chem. Heterocycl. Compd. (Engl. Transl.)* **1979**, *16*, 1097–1100.

(32) Khoshtariya, T. E.; Sikharulidze, M. I.; Kurkovskaya, L. N.; Suvorov, N. N. *Soobsh. Akad. Nauk Gruz. SSR* **1986**, *124*, 97–100.

(33) Pudlo, M.; Csányi, D.; Moreau, F.; Hajós, G.; Riedl, Z.; Sapi, J. First Suzuki−Miyaura type cross-coupling of *ortho*-azidobromobenzene with arylboronic acids and its application to the synthesis of fused aromatic indole-heterocycles. *Tetrahedron* **2007**, 10320–10329.

(34) Dagher, K.; Terent'ev, P. B.; Kulikov, N. S. Tetracyanoethylation and Fischer rearrangement of some 4-oxo-4,5,6,7-tetrahydroindoles. *Chem. Heterocycl. Compd. (Engl. Transl.)* **1986**, *22*, 172–175.

(35) Rawal, V. H.; Joes, R. J.; Cava, M. P. Palladium mediated dehydrogenation in the photochemical cyclization of heterocyclic analogs of stilbene. *Tetrahedron Lett.* **1985**, *26*, 2423–2426.

(36) Beccalli, E. M.; Marchesini, A.; Pilati, T. Synthesis of [*a*]annulated carbazoles from indol-2(3*H*)-one. *Synthesis* **1992**, 891–894.

(37) Fousteris, M. A.; Koutsourea, A. I.; Arsenou, E. S.; Leondiadis, A. L.; Nikolaropoulos, S. S.; Stamos, I. K. Pyrrolocarbazole analogs of aromatic skeleton of indolocarbazole natural products. *J. Heterocycl. Chem.* **2004**, *41*, 349–353.

(38) Remers, W. A.; Roth, R. H.; Gibs, G. J.; Weiss, M. J. Synthesis of indoles from 4-oxo-4,5,6,7-tetrahydroindoles. II. Introduction of substituents into the 4 and 5 positions. *J. Org. Chem.* **1971**, *36*, 1232–1240.

(39) Kakushima, M.; Hamel, P.; Frenette, R.; Rokach, J. Regioselective synthesis of acylpyrroles. *J. Org. Chem.* **1983**, *48*, 3214–3219.

(40) Bain, J.; Plater, L.; Elliott, M.; Shpiro, N.; Hastie, J.; McLauchlan, H.; Klervernic, I.; Arthur, S. C.; Alessi, D. R.; Cohen, P. The selectivity of protein kinase inhibitors: a further update. *Biochem. J.* **2007**, *408*, 297–315.

(41) Xu, D.-Q.; Yang, W.-L.; Luo, S.-P.; Wang, B.-T.; Wu, J.; Xu, Z.-Y. Fischer indole synthesis in Brønsted acidic ionic liquids: A green,

mild, and regiospecific reaction system. *Eur. J. Org. Chem.* **2007**, 1007–1012.
(42) Bullock, A. N.; Debreczeni, J. E.; Fedorov, O. Y.; Nelson, A.; Marsden, B. D.; Knapp, S. Structural Basis of Inhibitor Specificity of the Human Protooncogene Proviral Insertion Site in Moloney Murine Leukemia Virus (PIM-1) Kinase. *J. Med. Chem.* **2005**, *48*, 7604–7614.
(43) Debreczeni, J. E.; Bullock, A. N.; Atilla, E.; Williams, D. S.; Bregman, H.; Knapp, S. Meggers, E. Ruthenium Half-Sandwich Complexes Bound to Protein Kinase Pim-1. *Angw. Chem., Int. Ed.* **2006**, *45*, 1580–1585.
(44) Qian, K. C.; Wang, L.; Hickey, E. R.; Studts, J.; Barringer, K.; Peng, C.; Kronkaitis, A.; Li, J.; White, A.; Mische, S.; Farmer, B. Structural basis of constitutive activity and a unique nucleotide binding mode of human Pim-1 kinase. *J. Biol. Chem.* **2005**, *280*, 6130–6137.
(45) Holder, S.; Lilly, M.; Brown, M. L. Comparative molecular field analysis of flavonoid inhibitors of the PIM-1 kinase. *Bioorg. Med. Chem.* **2007**, *15*, 6463–6473.
(46) Davies, S. P.; Reddy, H.; Caivano, M.; Cohen, P. Specificity and mechanism of action of some commonly used protein kinase inhibitors. *Biochem. J.* **2000**, *351*, 95–105.
(47) Leslie, A. G. W.; Powell, H. *MOSFLM*; MRC Laboratory of Molecular Biology: Cambridge, 2007.
(48) Evans, P. *SCALA—Scale Together Multiple Observations of Reflections*; MRC Laboratory of Molecular Biology: Cambridge, 2007.
(49) McCoy, A. J.; Grosse-Kunstleve, R. W.; Storoni, L. C.; Read, R. J. Likelihood-enhanced fast translation functions. *Acta Crystallogr., Sect. D: Biol. Crystallogr.* **2005**, *61*, 458–464.
(50) Emsley, P.; Cowtan, K. Coot: model-building tools for molecular graphics. *Acta Crystallogr., Sect. D: Biol. Crystallogr.* **2004**, *60*, 2126–2132.
(51) Murshudov, G. N.; Vagin, A. A.; Dodson, E. J. Refinement of macromolecular structures by the maximum-likelihood method. *Acta Crystallogr., Sect. D: Biol. Crystallogr.* **1997**, *53*, 240–255.
(52) Painter, J.; Merritt, E. A. Optimal description of a protein structure in terms of multiple groups undergoing TLS motion. *Acta Crystallogr., Sect. D: Biol. Crystallogr.* **2006**, *62*, 439–450.